AN EVALUATION OF RE-VEGETATION ON STREAMBANK STABILITY AND EROSION

A Thesis

by

DESTINY RENE RUSSELL

Submitted to the Office of Graduate and Professional Studies of
Texas A&M University
in partial fulfillment of the requirements for the degree of

MASTER OF SCIENCE

Chair of Committee,	Robert Knight
Co-Chair of Committee,	Fouad Jaber
Committee Member,	Diane Boellstorff
Intercollegiate Faculty Chair,	Ronald Kaiser

May 2020

Major Subject: Water Management and Hydrological Science

ABSTRACT

An essential, natural process of a stream is the movement of sediment. However, the natural balance of sediment transport in a stream is seldom observed as a result of anthropogenic implications. An urbanizing stream can experience increased erosion rates from impervious surfaces increasing runoff and runoff velocity. Poor riparian vegetation is a top physical habitat stressor along creek corridors, affecting 25% of total stream miles within the nation. Planting and maintaining a native riparian vegetated buffer is a basic, cost effective method used by many successful stream restoration projects for best management practices (BMPs). The study performed analyzed the effectiveness of native revegetation to reduce erosion through different assessments. Two reaches along a moderately erodible section of Geronimo Creek in Seguin, TX were selected. One site was re-vegetated (treatment segment), and the other (control segment) was left in its current condition. The geomorphology of the stream evolved from a semi C (2018) to a full G stream (2019) indicating lateral migration. A Bank Erosion Hazard Index (BEHI) was analyzed using a two independent samples t-test resulting in a statistical difference between the treatment and control segment after the approximate 1-year study period. The treatment segment observed 0.68 metric tons of soil loss/year more than the control segment in the bank recession analysis. The average sediment load change for the treatment and control segments were 26% reduction and 50% increase, respectively. The vegetation modified critical shear stress exceeded the average bankfull shear stress by an excess of 4.37 kg/m^2 meaning that erosion should be reducing as a result of vegetation. Stable vegetation is a fundamental part of the solution for restoration of degrading streams. As concluded by the study of the different assessments used, replanted native vegetation effectively reduces sediment load after approximately one year of study. Two to three more years should be added to the study to better observe reduced erosion

and soil load reduction from well-established mature plants as the stream and its banks experience many types of storm frequencies and durations.

ACKNOWLEDGEMENTS

I would first like to give thanks to Jesus Christ my Savior for giving me the patience, determination, and thirst of knowledge to complete this degree and achieve an academic goal of mine. I am grateful for my husband who was my cheerleader, editor, statistics teacher, and counselor through what seemed like a never-ending emotional rollercoaster. For my family who supported, encouraged, and prayed for me through the entire process, especially my mom and dad who even helped plant vegetation out of pure interest in my study.

I would like to give thanks to Dr. Fouad Jaber for being a kind and personal professor, teaching me the basics of Natural Channel Design, the different assessments, and guiding me through the analysis of my study. To Nathan Glavy, Clare Entwistle, and Isabella Garrone for all their hard work and friendship. To Nikki Dictson and Lucas Gregory for their hard work and expertise, and to all other Texas Water Resources Institute staff for making the work place an enjoyable learning environment. To Dr. Diane Boellstorff and Dr. Robert Knight for being part of my committee and providing feedback and edits.

I would also like to thank the Irma Lewis Seguin Outdoor Learning Center, Guadalupe-Blanco River Authority, Texas Parks and Wildlife Department, and all volunteers who helped make this study possible.

CONTRIBUTORS AND FUNDING SOURCES

Contributors

This study was supported by a thesis committee consisting of Dr. Robert Knight of the Department of Ecosystem Science and Management as Chair, Dr. Fouad Jaber of the Department of Biological and Agricultural Engineering as Co-Chair, and Dr. Diane Boellstorff of the Department of Soil and Crop Sciences as committee member. The Irma Lewis Seguin Outdoor Learning Center allowed access and permission to hold the study at the Center. Guadalupe-Blanco River Authority performed the Total Suspended Solids analysis. Texas Water Resources Institute staff including Lucas Gregory, Clare Entwistle, Nathan Glavy, Nikki Dictson, and Isabella Garonne aided tremendously in equipment set-up, site maintenance, and data collection. Texas Parks and Wildlife Department and local nurseries gave expert advice on vegetation selection and planting techniques. Volunteers from different organizations came out and donated their time to the project.

Funding Sources

The study was made possible thanks to Texas Water Resources Institute, Texas Commission on Environmental Quality, Texas A&M AgriLife Research, and Texas A&M University.

NOMENCLATURE

ADCP	Acoustic Doppler Current Profiler
BEHI	Bank Erosion Hazard Index
BMP	Best Management Practice
FAC	Facultative
FACUP	Facultative Upland
FACW	Facultative Wetland
FEMA	Federal Emergency Management Agency
GBRA	Guadalupe-Blanco River Authority
NBS	Near Bank Stress
NCD	Natural Channel Design
NCEI	National Centers for Environmental Information
NELAP	National Environmental Laboratory Accreditation Program
NOAA	National Oceanic and Atmospheric Administration
OBL	Obligate
SOLC	Seguin Outdoor Learning Center
TPWD	Texas Parks and Wildlife Department
TSS	Total Suspended Solids
USDA NRCS	United States Department of Agriculture Natural Resources Conservation Service
US EPA	United States Environmental Protection Agency

TABLE OF CONTENTS

LIST OF FIGURES

LIST OF TABLES

Page

1. INTRODUCTION

One of the essential, natural processes of a properly functioning stream is the movement of sediment (Wohl et al., 2015). For example, the Colorado River formed the Grand Canyon over millions of years by the natural erosion and evolution process of a stream (Longwell 1946 and Lucchitta 2003). However, the natural balance of sediment transport in a stream is seldom observed as a result of anthropogenic implications (e.g. levees, channelization, dams, heavy grazing, urbanization, and farming) (Belmont et al., 2011; Swanson et al., 2017; Wohl et al., 2015). The addition of infrastructure and impervious cover within the past century has caused an unprecedented acceleration of erosion rates (Arnold et al., 1982). This change in land cover has resulted in an increase in water volume and velocity traveling through concrete lined or manicured drainage ditches to stream corridors (Henshaw and Booth 2000). The sheer force of water in these manipulated drainages are displayed in the aftermath of eroded, unstable streambanks, with lateral migration and downcutting streambed (Henshaw and Booth 2000), sometimes allowing for the disconnection of the floodplain (Doll et al., 2003).

Approximately 1 out of 6 miles of streams within the United States have been found to have an excess of sediments (US EPA 2016) stemming from continuous erosion of streambanks (Hargrove et al., 2010 and Lenhart 2018). Increased sediment loads cause numerous negative impacts to the riparian ecosystem, aquatic habitat, and downstream to reservoirs (Belmont et al., 2011 and Hargrove et al., 2010). Pollutants and nutrients (i.e. phosphorus) that are insoluble can chemically adsorb to sediment particles that are transported throughout a watershed further causing deleterious effects to water quality (Walling and Webb 1985). Visual assessment of impacted streambanks can show evidence of lost natural riparian habitat, land use, property value, and in extreme cases danger for human safety (Pimentel et al., 1995). The total approximate in-stream damage from erosion is $5 billion for the United States each year (Pimentel et al., 1995), with a minimum of $15 billion spent on stream restoration within the United States from 1990 to 2005 (Bernhardt et al., 2005).

Traditionally, engineers simply apply hard armoring or mechanical techniques (i.e. riprap, gabions, channelization) to manipulate and resolve problems without looking at the natural processes and functions of the channel (Smith et al., 2009). Traditional methods do not provide a viable long-term solution, can accelerate erosion and degradation (Doll et al., 2003), and damage the habitat of aquatic wildlife (Nagle 2007). An approach dominating the stream restoration field is the Natural Channel Design (NCD) which aims to rehabilitate the dimension, pattern, and profile of an unstable stream (Rosgen 1996 and 2009). The goal of NCD is to bring back the natural functioning processes of soil movement, hydrology, and ecology as opposed to focusing on one aspect such as reducing bank erosion with gabions as a solution (Nagle 2007; Rosgen 1996 and 2009; USDA NRCS 2007). This approach evaluates reference reaches which is the geometry from the stable upstream channel or a stable channel of similar classification located within the same region, to analyze and perform restoration on portions of an unstable stream (Doll et al., 2003; Ernst et al., 2010; Rosgen 1996, 2001, and 2009).

Since 1999, NCD projects and watershed initiatives along the Catskill Mountain tributaries that supply water to New York City have been successful allowing the city to opt out of buying a filtration plant valued at $8 million (Baldigo et al., 2008 and Nagle 2007). Monitoring in the tributaries also found a rise in wildlife species representation (Baldigo et al., 2008). Another study showed a refined ecosystem after restoration on the Lower Red River in Idaho, using NCD (Klein et al., 2007). Performing the holistic approach of the NCD can be costly with an approximation of $165/m for small rangeland tributaries or $2300/m for urban channels according to Nagle (2007). Planting riparian vegetation is a basic, cost effective method used by many successful stream restoration projects (Nagle 2007).

Studies show that vegetation is an important function of a riparian corridor by serving as reinforcement for streambanks (Beeson and Doyle 1995; Miller et al., 2014; Perucca et al., 2007; Polvi et al., 2014; Purvis and Fox 2016). Riparian vegetation is an active element that is closely coupled with stream geomorphology based on time and space of differing biomass densities allowing this interaction to alter the speed and shape of the evolution of a stream (Davies and Gibling 2011; Perucca et al., 2007; Polvi and Wohl 2013; Tal and Paola 2007).

Poor riparian vegetation and high amounts of riparian disturbance are the top physical habitat stressors along creek corridors, affecting 25% of total stream miles within the nation, and allowing destructive flooding and erosion (US EPA 2016). Erosional processes occur approximately five to six times more frequently on bare streambanks compared to vegetated streambanks (Bartley et al., 2008 and Beeson and Doyle 1995). Planting riparian vegetation produces a suite of riparian ecosystem services, and accordingly it is a best management practice (BMP) selected by many (Lowrance 1997 and Sweeney 2007).

Riparian vegetation provides roughness to the banks attenuating the energy of floodwater, lessening the amount of potential damage, and allowing further aquifer recharge (Blackport et al., 1995 and Swanson et al., 2017). The vegetation filters the floodwaters capturing sediments, nutrients, and debris removing these pollutants from the stream (Lowrance 1997; Miller et al., 2014; Swanson et al., 2017; Sweeney et al., 2007). The root structure of riparian vegetation act as interlocking fibers to provide a strong cohesion for the soil, reducing the critical shear stress along the banks (Beeson and Doyle 1995; Miller et al., 2014; Polvi et al., 2014; Purvis and Fox 2016).

McClain et al. (2011) performed a study on the Sacramento River in California that concluded native understory planting produced more ground cover and increased native species density compared to unplanted sites left to natural species colonization over an approximate 11 to 18-year study period. Another study performed by Ren et al. (2018), discovered that after five years of revegetation of the riparian area along the Three Gorge Dam Reservoir in China, the resulting increase in diversity of soil bacteria implied healthier soil quality. González et al. (2015) evaluated 169 restoration technique papers and found that the second common practice for riparian restoration world-wide was active planting which refers to planting or seeding vegetation. Lenhart et al. (2018) performed a survey among landowners resulting in planting and maintaining riparian buffer as preferred choices for sediment reduction versus restoring sinuosity and floodplain reconnection.

Planting and maintaining a riparian buffer are simple, cost-effective ways stakeholders can protect their riparian property, the health of their watershed, and the habitat of aquatic wildlife by slowing the acceleration of bank erosion and providing native vegetation that supplies several environmental services to the ecosystem (Nagle 2007; Lowrance 1997; Sweeney 2007). According to Rosgen 1996, 2001, and 2009, the recommended time to revegetate a degraded stream channel is before the evolution into a G classification where the stream begins to grow deeper leading to widening. A study has not been performed analyzing the effects of native revegetation as a BMP through differing assessments (i.e. Bank Erosion Hazard Index (BEHI), total suspended solids (TSS), and soil pin erosion rates).

2. BACKGROUND

As sediment particles are transported downstream, the larger particle class, known as bedload, tumbles along the streambed (Leopold and Emmett 1976). The smaller particle class that is transported downstream in the water column is known as TSS (Doll et al., 2003). As the gravitational force of water is guided by the banks and streambed slope, erosion and deposition occur allowing for a stream to migrate and continually evolve over geologic time (Doll et al., 2003).

Anthropogenic influences can upset the dynamic equilibrium of a stream and accelerate the overall evolution process (Rosgen 1996, 2001, 2009). When an urbanizing stream experiences increased erosion rates caused by impervious surfaces, too much water will cause a sediment starved stream to scour and erode the banks and streambed leading to incision and possible cutoff from the floodplain (Lane 1955). Likewise, if there is too much of a sediment load for the stream to transport from land cover change (i.e. farming or construction), without the use of BMPs the channel will deposit the sediment building the streambed up over time and altering the flow path for water, potentially resulting in avulsion (Lane 1955). Once a channel reaches the degradation or aggradation stage, it takes a substantial amount of time to recover (Rosgen 1996, 2001, 2009).

The purpose of this study was to classify an urbanizing stream reach and perform a comprehensive analysis of sediment loads and erosion rates to evaluate the effectiveness of replanting native vegetation along the streambank. To the knowledge of the author, there has been no study of this kind that analyzed sediment load, BEHI, and bank erosion using a revegetated segment against a control segment.

3. METHODS AND MATERIALS

3.1 Site Selection and Background

The study site is nestled within the Irma Lewis Seguin Outdoor Learning Center (SOLC) along Geronimo Creek approximately 3.7 km northeast of Seguin, Guadalupe County, Texas (Figure 3.1). The SOLC has ease of access to Geronimo Creek where the upland corridor on the left side of the stream, looking downstream, has a walking/biking path open to the public and is used as a stream walk for educating school kids about riparian and instream habitat.

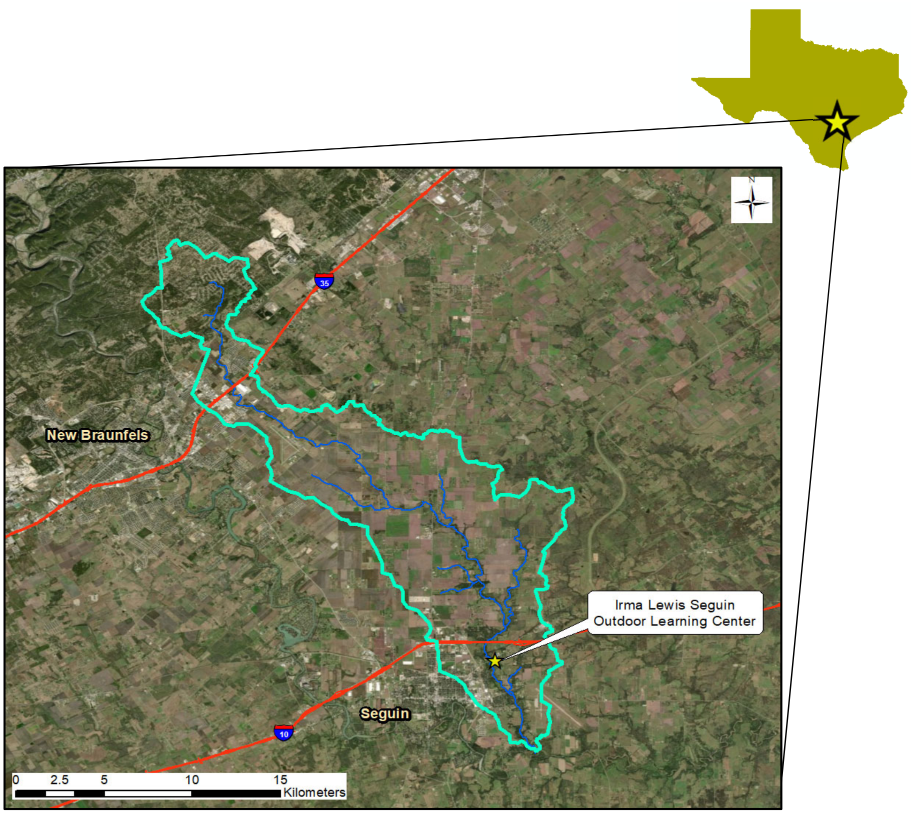

Figure 3.1 A map of Alligator and Geronimo Creeks watershed with the field site location at the SOLC. Source: Figure 3.1 map was created using ArcGIS® software by Esri. ArcGIS® and ArcMap™ are the intellectual property of Esri and are herein under license.

Within the greater basin of the Guadalupe River, the watershed of Geronimo Creek and its tributaries including Alligator Creek, Baer Creek, and numerous springs comprise approximately 181 km^2 (Geronimo Creek Watershed Data Report 2016).

Geronimo Creek is located within the gently sloping Blackland Prairie ecoregion found to have dark, calcareous clays of the Branyon soil series dominating the drainage area (USDA NRCS 1977). The riparian areas are comprised of species such as pecan tree (*Carya illinoinensis*), black willow (*Salix nigra*), black walnut (*Juglans nigra*), American sycamore (*Platanus occidentalis*), honey locust (*Gleditsia triacanthos*), buttonbush (*Cephalanthus occidentalis*), and Indian woodoats (*Chasmanthium latifolium*) (Texas A&M Forest Service 2018). There are several species of benthic macroinvertebrates in Geronimo Creek including mayflies (*Ephemeroptera*), beetles (*Coleoptera*), dragonflies (*Anisoptera*), and dobsonflies (*Megaloptera*) (Ling et al., 2012). Fish species including central stoneroller (*Campostoma anomalum*), Texas logperch (*Percina carbonaria*), largemouth bass (*Micropterus salmoides*), orangethroat darter (*Etheostoma spectabile*), and Texas shiner (*Notropis amabilis*) (Ling et al., 2012). A mild subtropical climate allows for a summer average high of 34.5° C and a winter average low of 5.8° C with an average precipitation of 80.87 cm annually (NOAA 2018).

The majority of the development surrounding Geronimo Creek shown in Figure 3.2, created by overlaying the National Land Cover Database 2016 developed by Yang et al., 2018, is a result of the growing populations of Seguin and New Braunfels with an increase of 13.2% and 37.1%, respectively, from 2010 to 2017 (United States Census 2017).

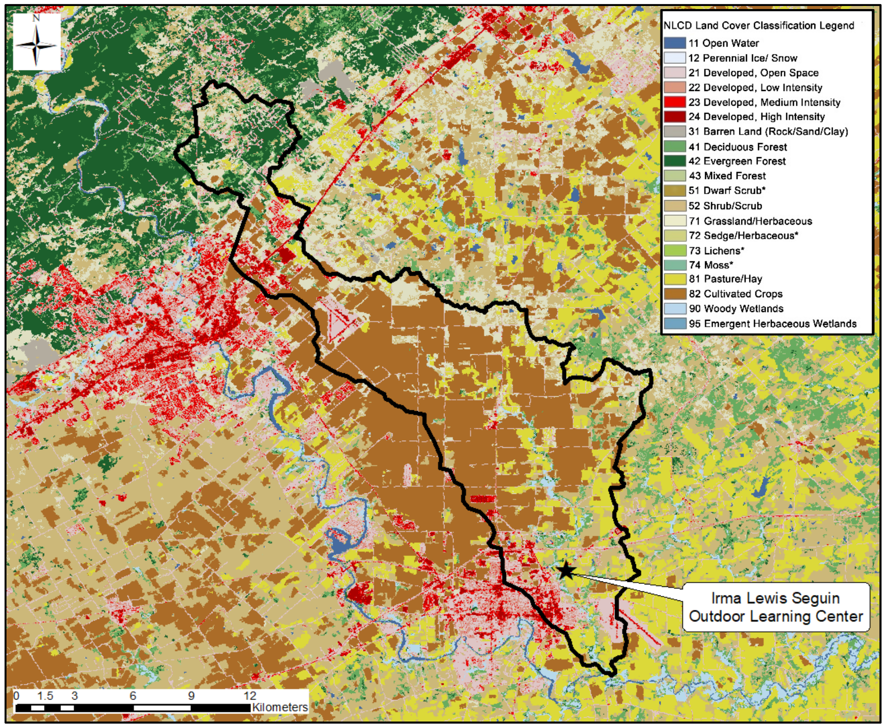

Figure 3.2 The land cover within and around the Alligator and Geronimo Creeks Watershed. Source: Figure 3.2 map was created using ArcGIS® software by Esri. ArcGIS® and ArcMap™ are the intellectual property of Esri and are herein under license. Copyright © Esri. All rights reserved.

Additionally, this growth can be influenced by the close proximities of fast-growing cities such as San Antonio, San Marcos, and Austin (Ling et al., 2012). Other changes in land cover within the majority of the watershed are the conversion to farmland where the major row crops include corn, sorghum, cotton, and oats or the conversion to pastureland for cattle and goat grazing (Ling et al., 2012). We chose the SOLC as the project site because of the land use changes, specifically urbanization, along with permission for and ease of access. Additionally, the Geronimo and Alligator Creeks Watershed has an approved watershed protection plan which was produced to address an identified bacteria impairment (Ling et al., 2012). The following methods performed on the project site are BMPs that will filter and thus reduce pollutants and sediments during flood events (Goel et al. 2004).

The area for the project is collectively 91.44 m in length. In Figure 3.3, the beginning 30.48 m located upstream was the restored/treatment segment where native vegetation was planted. The second 30.48 m was left untouched as a buffer. The last 30.48 m was located downstream as the control segment which did not receive any planting activities.

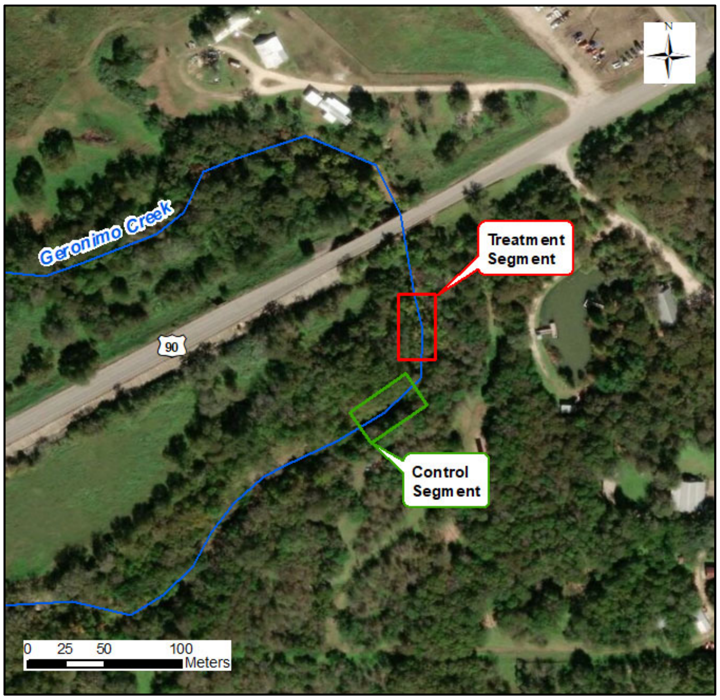

Figure 3.3 A map of Geronimo Creek zoomed in to the field site location showing the areas of treatment and control. Source: Figure 3.3 map was created using ArcGIS® software by Esri. ArcGIS® and ArcMap™ are the intellectual property of Esri and are herein under license. Copyright © Esri. All rights reserved.

The arrangement of the treatment segment before the control segment was selected as a result of limited streambank access and minimal area to perform treatment activities within the control area. Revegetation of the treatment segment will be compared to the control segment to provide data on bank erosion and sediment loading. The arrangement will not affect the results of the project as monitoring of sediment loads will occur at the beginning and end of each segment.

The project began in March of 2018 with data collection ranging from July of 2018 to May of 2019.

3.2 Revegetation

The treatment segment had several existing native trees and shrubs with the majority of ground cover comprised of non-native St. Augustinegrass (*Stenotaphrum secundatum*). Upon completion of a site visit, Texas Parks and Wildlife Department (TPWD) and local nurseries recommended several native species for the treatment segment that would tolerate partial shade while stabilizing streambanks with fast and strong root colonizing characteristics. In March of 2018, jutte matting was staked across the banks of the treatment segment. The matting was biodegradable and used to prevent erosion in the early stages of plant establishment. The majority of the area was planted with several varieties of grasses, sedges, and rushes listed in Table 3.1. As recommended, the vegetation was planted among the St. Augustine grass in order to shade out the non-native versus removing it. As a result of the short-term project, bare root and potted vegetation were planted versus broadcasted seed.

The vegetation was planted according to a rating used to distinguish the wet/dry conditions that the plant will survive in based on wetland areas. Vegetation that were rated obligate (OBL) and facultative wet (FACW) species were mostly bare root planted along a swath of area approximately 0.61 m up the streambank along the creek's edge. The OBL and FACW species survive on inundated to frequently flooded soils. The plants were planted in a triangular format with 10 to 15 cm of space between each plant. Facultative (FAC) plants were planted further up the streambank where the soil is less frequently flooded. A mixture of FAC and Facultative Upland (FACUP) species were planted along the upland portions of the streambank along the walking/biking trail where flooding occurs more infrequently. The FAC and FACUP species were mostly potted plants that were planted in a triangular pattern 15 to 30 cm in spacing depending on size.

Table 3.1 A list of the native vegetation that was planted along the riparian corridor in the treatment segment along Geronimo Creek.

Common Name	Scientific Name	Wetland Status
creek sedge	*Carex amphibola*	FACW
stream sedge	*Carex blanda*	FAC
Cherokee sedge	*Carex cherokeensis*	FACW
Emory's sedge	*Carex emoryi*	OBL
Leavenworth's sedge	*Carex leavenworthii*	UPL
inland sea oats	*Chasmanthium latifolium*	FAC
roughleaf dogwood	*Cornus drummondii*	FAC
creeping spikerush	*Eleocharis montevidensis*	FACW
beaked spikerush	*Eleocharis rostellata*	OBL
scouringrush horsetail	*Equisetum hyemale*	FACW
purple lovegrass	*Eragrostis spectabilis*	FACUP
cardinalflower	*Lobelia cardinalis*	FACW
Turk's cap	*Malvaviscus arboreus*	UPL
frog fruit	*Phyla nodiflora*	FAC
obedient plant	*Physostegia virginiana*	FACW
Texas blue grass	*Poa arachnifera*	UPL
white star sedge	*Rhynchospora colorata*	FACW
black willow	*Salix nigra*	OBL
purpletop tridens	*Triden flavus*	FACUP
eastern gamagrass	*Tripsacum dactyloides*	FAC

Five days after the planting, a significant storm moved through the area producing a flood that overtopped the banks and washed away several of the newly planted vegetation types. Due to late spring planting and a dry summer, the plants were watered through August. After a permit was obtained by the local Guadalupe-Blanco River Authority, invasive non-native elephant ears (*Colocasia esculenta*) were hand-pulled and sprayed using a 7.5-L hand pump sprayer for suppression in both the treatment and control segments using Clearcast (1%) and Dyne-Amic (0.8%) herbicide mixture. Removing the elephant ears enabled native species to move in and establish. In early October 2018, a second round of planting occurred to fill in the gaps where plants were washed away earlier in the project.

3.3 Geomorphology

The annual geomorphological data for the years 2018 and 2019 for Geronimo Creek were assessed similar to the recommendations of Doll et al., 2003. Four permanent cross sections were established in the treatment and control segments for a total of eight cross sections. One cross section was located at the beginning of the segment, two cross sections were evenly spaced in the middle of the segment, and one cross section was located at the end of the segment.

DeWalt® laser level surveying equipment was used to survey the cross sections. The laser level was set at a level elevation in the treatment segment at a height that visibly allowed for elevation data to be obtained throughout the four cross sections. A permanent point in the treatment segment was used as the back-sight which was taken as a benchmark for an arbitrary elevation of 30.5 m. The back-sight was measured using the laser level receiver attached to the top of a measuring rod that extended until the laser level made connection with the receiver denoted by a constant beep sound. Once the back-sight was measured, points located every 0.3 m along the permanent cross section, perpendicular to the stream, were measured. Other specific points were noted along the cross section that included the top of bank, bankfull stage, thalweg, and edge of water. Bankfull stage is the point at which the water level begins to flow out of the banks and into the floodplain while the thalweg is identified the deepest part of the creek. Once each cross section in the treatment segment was measured, a turning point was taken to another laser level located within the control segment as a result of distance. The elevation data for the control segment was then measured. Once data elevation was obtained, geomorphic parameters were calculated (e.g. the area at bankfull, width at bankfull, width of flood prone area, maximum depth at bankfull, maximum depth from top of low bank, mean depth at bankfull entrenchment ratio, width to depth ratio, bank height ratio, and maximum depth ratio).

The same survey procedure was performed to obtain elevation data for the longitudinal profile from the beginning to the end of the project area that included the buffer segment in increments of 6 m along the thalweg. The longitudinal profile data was used to calculate the slope or elevation change of the channel for the entire project area and the individual treatment and control segments. The valley length and stream length for a long section of the stream that included the demonstration area were measured in Google Earth™ and used to calculate sinuosity. The sinuosity of the stream is calculated as

$$Sinuosity = Stream\ Length/Valley\ Length \qquad \text{(eq. 3.1)}$$

Wolman pebble counts (Wolman 1954) were conducted for each cross section. The pebble counts were performed by stringing a measuring tape, perpendicular to stream, from bankfull to bankfull and dividing the bankfull width by 100 in order to obtain 100 evenly spaced data samples. At every evenly spaced sample increment along the measuring tape, without looking, the first pebble touched was picked up and measured. The same technique was used to count pebbles for the longitudinal length of the stream by collecting 12 to 13 pebble counts per cross section to total 100 samples for the entire reach. The pebble counts were used to classify each cross section and the longitudinal reach based on dominant (D_{50}) substrate material. The same pebble count technique was performed from water's edge to water's edge for the riffle at cross section 1 upstream in the treatment segment and used in calculating sediment competency.

Rosgen's Classification of Natural Rivers Key assigns a letter and number to a stream's geomorphology based on entrenchment ratio, width/depth ratio, sinuosity, slope, and channel material (Rosgen 1996 and 2009). The data from the geomorphological measurements were used to classify the stream and compare the data from 2018 to 2019. The comparison determined any change in the geomorphology and evaluated how effective revegetation is to streambank stabilization.

3.4 Bank Erosion Hazard Index

BEHI is an assessment of the erosion potential of streambanks that was created by Rosgen (1996, 2001, 2009). The assessment evaluates the different characteristics of a streambank's condition by assigning point values and calculating an overall score. The characteristics of a streambank that affect the degree of erosion include: bank height vs bankfull depth, bank angle, density of roots, percentage of bank surface protection, root depth ratio, soil stratification, and particle size. Each of these characteristics are assigned a value based on measurement or appearance, which correlates to an index of very low to extreme. The characteristic indices are then totaled to identify the overall hazard of erosion (Table 3.2).

Table 3.2 Rosgen's BEHI rating for the total characteristic indices.

Index	Hazard
5 - 9.5	Very Low
10 - 19.5	Low
20 - 29.5	Moderate
30 - 39.5	High
40 - 45	Very High
46 - 50	Extreme

The BEHI was performed for each bank in each cross section quarterly from the beginning of the study to the end of the study. A two independent samples t-test was performed to evaluate the BEHI change or difference from the beginning of the study to the end of the study in each segment. The analysis of change will show if planted native riparian revegetation is an effective BMP in the study.

3.5 Near Bank Stress

The Near Bank Stress (NBS) assessment rates the amount of energy that is distributed against a bank (Rosgen 2001 and 2009). The assessment variables depict probable energy distribution that is disproportionate in the near-bank zone which leads to increased erosion of a streambank. The near-bank zone is located within the 1/3 bankfull width of the evaluated bank. There are seven different ways to measure NBS. Method 1 is reconnaissance; Methods 2, 3 and 4 are general predictions; Methods 5 and 6 are detailed predictions and Method 7 is validation. For the purpose of this study, Methods 5 and 6 were selected to perform NBS since Method 7 required detailed, time consuming measurements. The assessment was performed at the end of the one-year study with the resulting highest NBS rating used. Method 5 calculates the ratio of near-bank maximum depth (d_{nb}) to the average bankfull depth (d_{bkf}) shown in eq. 3.2.

$$NBS = \frac{d_{nb}}{d_{bkf}} \qquad \text{(eq. 3.2)}$$

Method 6 calculates the ratio of the near-bank shear stress (τ_{nb}) to bankfull shear stress (τ_{bkf}) shown in eq. 3.3 – 3.5

$$\tau_{nb} = \gamma \times d_{nb} \times S_{nb} \qquad \text{(eq. 3.3)}$$

$$\tau_{bkf} = \gamma \times d_{bkf} \times S \qquad \text{(eq. 3.4)}$$

$$NBS = \frac{\tau_{nb}}{\tau} \qquad \text{(eq. 3.5)}$$

where γ is the specific gravity of water at 304.66 kg/m^2, d_{nb} is the near-bank maximum depth, S_{nb} is the near-bank water surface slope, d_{bkf} is the average depth at bankfull, and S is the average water surface slope. The NBS value is then rated on a scale from very low to extreme.

3.6 Precipitation

Precipitation data from September 2018 through May 2019 was downloaded from 11 National Centers for Environmental Information (NCEI) gauges within or near the Geronimo Watershed. Thiessen polygons were created, using QGIS ® and ArcGIS ® by ESRI ™, to calculate the weighted average rainfall for the overall watershed. The weighted rainfall average was calculated using

$$\overline{P} = \frac{P_1A_1 + P_2A_2 + P_3A_3 + \ldots + P_nA_n}{A_1 + A_2 + A_3 + \ldots + A_n} = \frac{\sum_{i=1}^{n} P_iA_i}{\sum_{i=1}^{n} A_i} \qquad \text{(eq. 3.6)}$$

where the weighted average is $\overline{P}$, precipitation measurements from each gauge are the P's, and the area of each associated polygon are the A's.

Geronimo Creek is referred to as being a "flashy" system, rising and receding quickly after large storm events within the watershed. To quantify the flashiness of a river, Baker et al. (2004) developed the Richards-Baker Flashiness Index (R-B Index) which is a modified equation of the Richards Pathlength developed by Gustafson et al. (2004). The R-B Index measures discharge oscillations with respect to total discharge which portrays the way a watershed processes hydrological inputs into the streamflow outputs (Baker et al., 2004). The following R-B Index (eq. 3.7) was used to determine the flashiness of Geronimo Creek.

$$\textit{R-B Index} = \frac{\sum_{i=1}^{n} |q_i - q_{i-1}|}{\sum_{i=1}^{n} q_i} \qquad \text{(eq. 3.7)}$$

The daily discharge volume in cubic meters per second is represented by q. Depending on the size range of the watershed area, a low index value represents stable streams while a high index value represents flashy streams on the continuum.

3.7 Total Suspended Solids

TSS samples were gathered during storm event-based monitoring from July 2018 through May 2019. To collect composite storm samples, four Teledyne ® ISCO Model 6712 automated water samplers were installed above the floodplain. Each ISCO received an identification number that started in order from upstream, ISCO 22026, to downstream, ISCO 22029 (Figure 3.4).

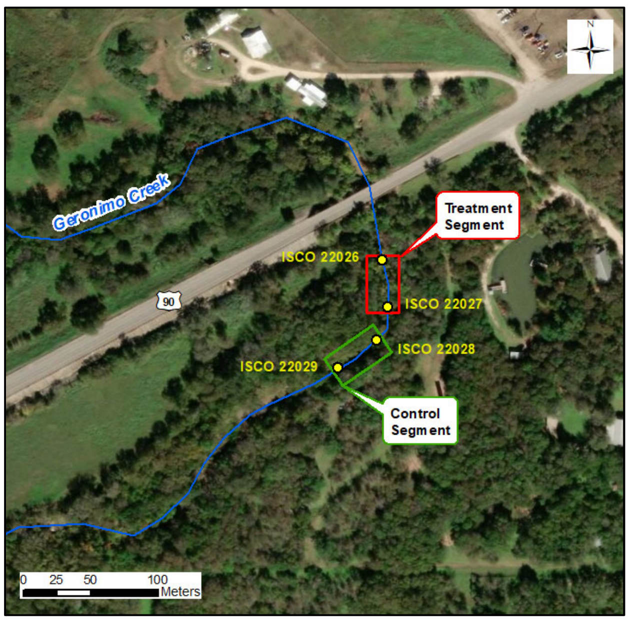

Figure 3.4 A map of the field site location showing the areas of treatment and control with placement of the ISCO automated water samplers. Source: Figure 3.4 map was created using ArcGIS® software by Esri. ArcGIS® and ArcMap™ are the intellectual property of Esri and are herein under license. Copyright © Esri. All rights reserved.

Each sampler was housed, powered by a solar panel, and connected to two field lines (bubbler and strainer) that ran into the stream at a fixed location, approximately 1/3 depth from the bottom of the creek bed, near the beginning and end of each segment. The samplers recorded water depth using ISCO Model 730 bubbler flow modules. ISCO sampler 22029 was calibrated to estimate flow (cms) using Manning's equation (Chow 1959) represented as

$$Q=VA=(1.49/n)AR^{2/3}\sqrt{S} \qquad \text{(eq. 3.8)}$$

where Q is flow rate, V is velocity, A is flow area, n is Manning's roughness coefficient, R is hydraulic radius, and S is channel slope. This calculation is enabled by programming the stream's channel dimensions into the ISCO 6712 sampling unit and depth of water recorded by the bubbler. As depth changes, the area of the stream cross section and hydraulic radius change thus affecting the calculated flow result. A SonTek RiverSurveyor® M9 Acoustic Doppler Current Profiler (ADCP) was deployed once to gather average discharge data from the permanent cross sections. The average discharge for the respective cross section was then used to calculate n, Manning's roughness coefficient from eq. 3.8.

Data was recorded internally on the ISCO 7612 sampler at 10-minute intervals. The samplers were programmed to remain idle, recording the depth level of the creek until a certain programmed water level was reached. This programmed level, called the trigger point, was set to obtain samples when the volume of runoff from a storm produced 2.54 cm or more of precipitation within the watershed. The trigger level corresponded to 0.06 m or 0.12 m above the seasonal ambient depth. For the Geronimo Creek watershed area, the normal wet seasons are early fall and late spring (Arguez et al., 2012).

When the trigger point was reached or exceeded, the samplers would turn on and collect a 1,000 ml sample of creek water every hour until either a 20 L bottle was full or the creek level fell below the trigger point again. Within a 24-hour to 48-hour time period, the samples were placed on ice and taken to the Guadalupe-Blanco River Authority Laboratory (GBRA) in Seguin, Texas for analysis of TSS using method 2540 D (Baird et al., 2017), which is the standard operating procedure for TSS. The holding time for TSS was seven days. GBRA is a National Environmental Laboratory Accreditation Program (NELAP) recognized laboratory.

The TSS concentration results from the GBRA lab were then used to calculate the load and load reduction of the treatment segment compared to the control segment using

$$TSS\ Load\ (kg/event) = a * b * c \qquad \text{(eq. 3.9)}$$

$$Load\ Reduction\ (\%) = \left(\frac{average\ ending\ segment - average\ beginning\ segment}{average\ beginning\ segment}\right) * 100 \qquad \text{(eq. 3.10)}$$

where *a* is the TSS concentration (mg/L), *b* is the discharge (m^3/s), and *c* is the amount of seconds passed during the storm event.

3.8 Annual Recession Rate

Erosion pins were used as a way of measuring the lateral migration of each bank for each cross section. The erosion pins were made of 0.9 m long rebar with 15 cm at one end spray painted fluorescent orange. The pins located at 0.3, 0.9, and 1.5 m above the normal water level were installed perpendicular to the bank surface exposing only the painted 15 cm. The erosion pins were measured quarterly and then pounded back into the bank until only the painted 15 cm were seen again. The observed erosion rates from the erosion pins were used to calculate the estimated annual recession rate or soil loss of the banks, in tons of soil per year, using

$$Estimated\ Soil\ Loss = \frac{a*b*c*d}{907} \qquad \text{(eq. 3.11)}$$

where *a* is eroding bank length (m), *b* is eroding bank height (m), *c* is the lateral recession rate (m/yr), and *d* is soil weight (kg/m^3).

3.9 Sediment Competency and Critical Shear Stress

To obtain the sediment competency of the stream reach, a wet perimeter pebble count and bar sample were performed (Doll et al., 2003). The Wolman pebble count method, as previously mentioned, was performed at the riffle located at treatment 1 cross section. The pebble count was used to obtain a representative D_{50} of the cross section from the left edge of water to the right edge of water. The bar sample was excavated at the bottom 1/3 of a well-established point bar located adjacent to the riffle at treatment 1 cross section. The bar sample was taken adjacent to the edge of water where there was representative sample of the entire point bar material. A bottomless 20-L bucket was placed on the representative sample. The top two largest particles were selected and the intermediate axis was measured. The largest particle represents d_i. The bucket was pushed into the material at a depth twice that of the intermediate axis of the largest particle and placed in a bag for wet sieving.

The bagged excavated material was brought to the lab for wet sieving using 2.0, 4.0, 8.0, 16.0, 31.0, 5.0, and 63.0-mm sieves. Stacked from largest millimeter sieve on top to smallest millimeter sieve on bottom, the excavated material was agitated with a medium to low water pressure from a tap faucet and sifted through the tower of sieves where the particles smaller than 2.0 mm were caught by a 20-L bucket. Once all material was sieved by class size and the catch bucket drained of excess water, each class size was placed in brown paper bags with the class size less than 2.0 mm placed in a tared 1,000 ml metal beaker. The samples were placed in a Blue M® STABIL-THERM Gravity Oven and dried until a constant weight was reached for three hours at 60° C. After drying, each class size and the top two largest surface particles were placed in a tared metal pan and weighed with a Fisher Science Education™ digital scale. The weight and size of the top two largest surface particles were used to determine material size class distribution.

Critical shear stress measures the amount of force needed to capture sediment of a particular size class and transport it downstream. The D_{50} for the substrate in the riffle located at treatment 1 cross-section was used to obtain the corresponding critical shear stress utilizing

Shield's Diagram (Leopold 1994). The calculated critical shear stress does not consider vegetation along the banks. To account for vegetation, a critical shear stress coefficient of 5.40 designated for sparse trees (Julian & Torres 2006) was multiplied by the calculated critical shear stress to result in a vegetation modified critical shear stress. Shear stress is the force of streamflow exerted on the stream bed and bank. The shear stress of the stream was calculated using

$$\tau = \gamma RS \qquad \text{(eq. 3.12)}$$

where τ is shear stress (kg/m^2), γ is the density of water (999.55 kg/m^3), R is the hydraulic radius of the riffle cross-section at bankfull stage (m), and S is the average stream slope. If the critical shear stress exceeds shear stress, erosion is reduced (Julian & Torres 2006). If the critical shear stress does not exceed the shear stress, erosion is increased (Julian & Torres 2006).

4. RESULTS

4.1 Revegetation

One year after planting and maintenance, several species started taking root, spreading, and flourishing in the treatment segment as shown in Figure 4.1. After a large storm in December, the wood pile was washed away and by April of 2019 vegetation began to encroach on the bare ground. In the control segment, very little change was observed as shown in Figure 4.2. Spraying of the invasive elephant ears in both segments opened up the bank to for native plants to spread and establish. The right control bank did not have any change overall. The right treatment bank, similar to the left, increased in herbaceous cover after one year as observed in Figure 4.3.

Figure 4.1 Left photo was taken in March of 2018 while right photo was taken in April of 2019 in the treatment segment of the left bank.

Figure 4.2 Left photo was taken in March of 2018 while right photo was taken in April of 2019 in the control segment of the left bank.

Figure 4.3 Left photo was taken in April of 2018 while right photo was taken in April of 2019 in the treatment segment of the left bank.

4.2 Geomorphology

The sinuosity of the stream for a long section of Geronimo Creek that included the demonstration area resulted in a calculated overall sinuosity of 1.9 (Figure 4.4). The average slope of the stream for the 2018 data at the demonstration site was 0.007 or (0.7%). The treatment segment was steeper than the control segment, but both had relatively mild slopes smaller than 0.02 (or 2%).

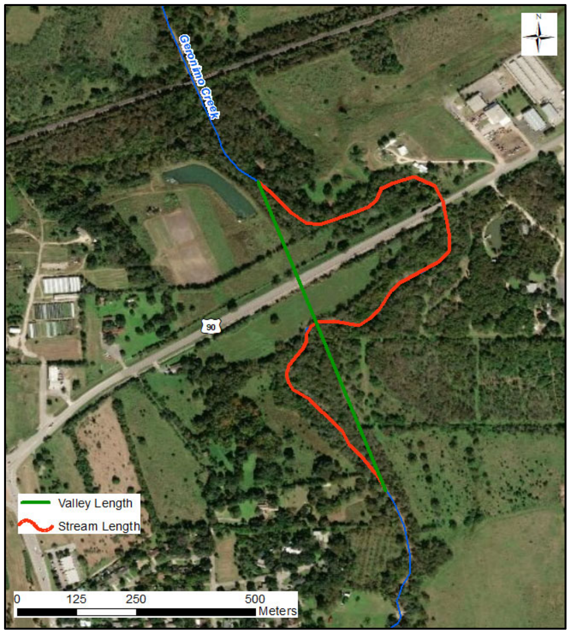

Figure 4.4 Stream length and valley length shown for a section that includes the study site within Geronimo Creek in Seguin, TX.

The upstream section had 2 cross sections that classified as C6 while the other two were either a G6c or an inconclusive classification (Table 4.1). The 4 cross sections downstream indicated a G6c stream.

Table 4.1 2018 stream classification parameters derived from geomorphological measurements.

Cross Section	Entrenchment Ratio	Width/Depth Ratio	Sinuosity	Stream Type	Slope	Channel Material	
Treatment 1	1.45	12.6	1.9	G	0.007	gravel	4c
Treatment 2	2	31.1	1.9	C	0.007	inconclusive	6
Treatment 3	2.3	16.7	1.9	C	0.007	inconclusive	6
Treatment 4	1.6	8.8	1.9	G	0.007	silt/clay	6c
Control 1	1.3	12.1	1.9	G	0.007	silt/clay	6c
Control 2	1.3	9.3	1.9	G	0.007	silt/clay	6c
Control 3	1.3	8.6	1.9	G	0.007	silt/clay	6c
Control 4	1.2	9.1	1.9	G	0.007	silt/clay	6c

The average slope of the stream for the 2019 data at the demonstration site was found to be 0.009 or (0.9%). The treatment segment was steeper than the control segment, but both had relatively mild slopes smaller than 0.02 (or 2%). Both segments classified as a G stream with the dominant substrate being gravel (Table 4.2).

Table 4.2 2019 stream classification parameters derived from geomorphological measurements.

Cross Section	Entrenchment Ratio	Width/Depth Ratio	Sinuosity	Stream Type	Slope	Channel Material	
Treatment 1	1.5	13.4	1.9	G	0.009	gravel	4c
Treatment 2	1.2	13.2	1.9	G	0.009	gravel	4c
Treatment 3	1.4	10	1.9	G	0.009	silt/clay	6c
Treatment 4	1.5	7.1	1.9	G	0.009	silt/clay	6c
Control 1	1.4	8.3	1.9	G	0.009	gravel	4c
Control 2	1.3	9.8	1.9	G	0.009	gravel	4c
Control 3	1.2	6.4	1.9	G	0.009	bedrock	1c
Control 4	1.3	6.2	1.9	G	0.009	bedrock	1c

4.3 Bank Erosion Hazard Index

The BEHI ratings for each quarter across each bank cross section assessment of bank height to bankfull height, root depth to bank height, root density, bank angle, surface protection, and bank material were totaled and are shown in Table 4.3.

Table 4.3 Results of the BEHI assessment for each bank cross section performed quarterly throughout the study period.

Segment Type	Cross Section #	3/12/2018 BEHI Rating	10/26/2018 BEHI Rating	1/10/2019 BEHI Rating	4/26/2019 BEHI Rating
Treatment Left	1	mod	mod	mod	mod
	2	low/mod	low	low	low
	3	mod	low	low	low
	4	mod	mod	mod	low
Treatment Right	1	low/mod	low/mod	low/mod	low
	2	mod	mod	mod	low
	3	mod	mod	mod	mod
	4	mod	mod	mod	low/mod
Control Left	1	high	high	high	high
	2	high	high	high	high
	3	high	high	high	high
	4	mod/high	high	high	high
Control Right	1	mod	mod	mod	mod
	2	mod	mod	mod	mod
	3	mod	mod	mod	mod
	4	mod	mod	mod	mod

A two independent samples t-test was performed using the change or difference in BEHI values from the beginning to end of project for the control segment versus the treatment segment. The test was executed using Program R (v3.4.0; R Development Core Team 2017). The treatment segment (n = 8) had a mean of -2.075 with a standard deviation of 1.49. The control segment (n = 8) had a mean of -0.7 with a standard deviation of 1.29. Overall, the change in the BEHI index and rating for the treatment segment improved while the control segment had little to no change. The test resulted in a p-value of 0.06845 meaning there was a statistical difference in the change of BEHI values from the control to the treatment segments at the $p<0.10$ level (Figure 4.5).

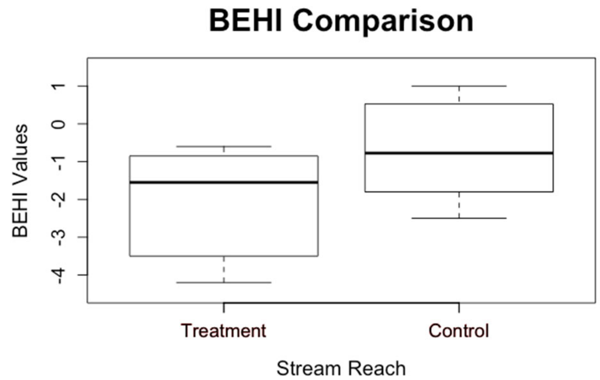

Figure 4.5 Two independent samples t-test for the change in the control segment versus the treatment segment with statistical difference at the p<0.10 level.

4.4 Near Bank Stress

NBS for each cross-section bank resulted in an extreme rating for 13 out of the 16 cross sections (Table 4.4). For these sections, the energy is not evenly dispersed among the near bank resulting in an extreme rating for potential erosion to occur. The control left bank 1 which had a low rating and control left bank 3 and 4 which had a very low rating had more evenly distributed amounts of energy across the near bank area allowing for a low possibility of soil erosion to occur providing for a more stable bank.

Table 4.4 Results of the NBS Rating for each cross section using Methods 5 and 6.

Segment Type	Cross Section #	NBS Rating
Treatment Left	1	Extreme
	2	Extreme
	3	Extreme
	4	Extreme
Treatment Right	1	Extreme
	2	Extreme
	3	Extreme
	4	Extreme
Control Left	1	Low
	2	Extreme
	3	Very Low
	4	Very Low
Control Right	1	Extreme
	2	Extreme
	3	Extreme
	4	Extreme

4.5 Precipitation

There was a total of 12 storm events that produced near to or more than 2.54 cm of rainfall between July of 2018 and May of 2019. The majority of the storm events happened in fall and late spring with a couple of large storm events in the winter. Figure 4.6 shows an example of the Thiessen polygon used to obtain the average watershed rainfall.

Figure 4.6 Example of the Thiessen polygon used to calculate the weighted average of Alligator and Geronimo Creek Watershed using precipitation gauges from the storm event on May 6, 2019.

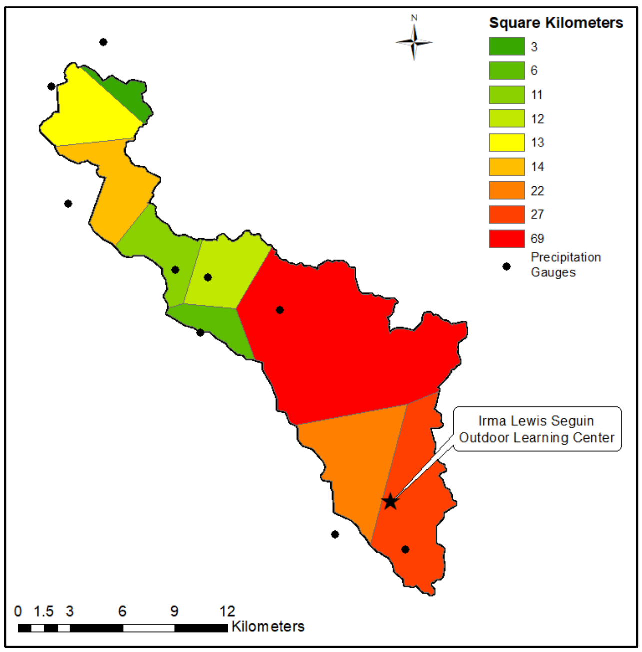

The largest storm event happened in December and precipitated 7.70 cm producing a discharge of 25.37 cms and a water level rise of 2.26 m (Table 4.5).

Table 4.5 Discharge, rainfall, and water level rise from stormwater sampling for the Alligator and Geronimo Creeks Watershed during the study period.

Monitoring Type	Storm Sample Date	Discharge (cms)	Weighted Average Rainfall (cm)	Average Water Level Rise (m)
Storm	9.10.18	2.97	4.14	0.44
Storm	9.13.18	8.75	4.85	1.02
Storm	9.17.18	5.04	6.32	0.68
Storm	9.25.18	0.64	2.21	0.07
Storm	10.11.18	0.68	3.33	0.08
Storm	10.16.18	9.21	5.61	1.06
Storm	10.26.18	0.95	2.84	0.12
Storm	12.11.18	25.37	7.70	2.26
Storm	1.03.19	13.85	2.74	1.42
Storm	4.08.19	2.15	4.52	0.30
Storm	4.18.20	1.76	3.38	0.24
Storm	5.6.19	6.71	6.17	0.73

The R-B Index value for Geronimo Creek resulted in an index of 0.50. Based on the study performed by Baker et al. (2004), Geronimo Creek is moderately flashy as a result of watershed size.

4.6 Total Suspended Solids

The measured TSS results for each storm event are shown in Table 4.6.

Table 4.6 TSS concentrations per storm event retrieved from ISCOs during the study period from July 2018 through May 2019.

Storm Sample Date	Discharge (cms)	Rainfall (cm)	Duration (seconds)	22026	22027	22028	22029
				TSS (mg/L)			
9.10.18	2.97	4.14	15600	49.7	133	75.4	150
9.13.18	8.75	4.85	21600	88.3	212	217	181
9.17.18	5.04	6.32	36000	124	107	98	169
9.25.18	0.64	2.21	14400	11.8	10.3	N/A	N/A
10.11.18	0.68	3.33	60600	17.3	34.3	25.8	28
10.16.18	9.21	5.61	48000	215	217	168	223
10.26.18	0.95	2.84	102600	14.1	14.8	12.8	N/A
12.11.18	25.37	7.70	91800	193	94.8	N/A	64.7
1.03.19	13.85	2.74	49800	176	202	82	178
4.08.19	2.15	4.52	19200	64.2	76	102	108
4.18.20	1.76	3.38	9600	46.4	54	84.8	32
5.6.19	6.71	6.17	46200	129	102	N/A	133

***N/A: Proper measurements were not retrieved as a result of ISCO malfunction.**

As described in eq. 3.9 (p. 19), the data were normalized based on the number of seconds for the individual storm duration. Table 4.7 shows the results of the load calculations for each ISCO in each storm. The average sediment load for ISCO 22026 and 22027 in the treatment segment were 0.062759 kg/event and 0.046696 kg/event, respectively. The average sediment load for ISCO 22028 and 22029 in the control segment were 0.024980 kg/event and 0.037420 kg/event, respectively.

Table 4.7 Sediment load per storm event during the study period from July 2018 through May 2019.

Storm Event	22026	22027	22028	22029
	Sediment Load (kg/event)			
9.10.18	0.00231	0.00617	0.00350	0.00696
9.13.18	0.01669	0.04007	0.04101	0.03421
9.17.18	0.02250	0.01942	0.01778	0.03067
9.25.18	0.00011	0.00009	N/A	N/A
10.11.18	0.00071	0.00141	0.00106	0.00115
10.16.18	0.09509	0.09598	0.07430	0.09863
10.26.18	0.00138	0.00145	0.00125	N/A
12.11.18	0.44952	0.22080	N/A	0.15070
1.03.19	0.12137	0.13929	0.05655	0.12274
4.08.19	0.00265	0.00314	0.00421	0.00446
4.18.20	0.00078	0.00091	0.00143	0.00054
5.6.19	0.04000	0.03163	N/A	0.04124

***N/A: Proper measurements were not retrieved as a result of ISCO malfunction.**

Table 4.8 shows the sediment load reduction for both segments for each individual storm event. Increase and reduction of sediment load was observed in both segments in differing storm events portraying noncorrelated measurements.

Table 4.8 Treatment and control percent reduction from the individual storm events.

Storm Event	Sediment Load Reduction (%)	
	Treatment	Control
9.10.18	168	99
9.13.18	140	-17
9.17.18	-14	72
9.25.18	-13	N/A
10.11.18	98	9
10.16.18	1	33
10.26.18	5	N/A
12.11.18	-51	N/A
1.03.19	15	117
4.08.19	18	6
4.18.20	16	-62
5.6.19	-21	N/A

***N/A: Proper measurements were not retrieved as a result of ISCO malfunction.**
****(+) number refers to increase in sediment load, and (-) number refers to decrease in sediment load.**

The average sediment load change for the treatment and control segments were 26% reduction and 50% increase, respectively. Therefore, the treatment segment on average decreased in sediment load while the control segment on average increased in sediment load.

4.7 Annual Recession Rate

During the study, the erosion recession for the treatment segment left bank produced 1.270 metric tons/year while the treatment segment right bank produced 0.591 metric tons/year (Table 4.9). The control segment left bank produced 1.098 metric tons/year, and the control segment right bank only produced 0.082 metric tons/year. The treatment segment eroded a total of 1.861 metric tons of soil/year. The control segment eroded a total of 1.180 metric tons of soil/year.

Table 4.9 Total recession rate of the study period for each bank of each segment.

Increment Above Normal Water Level (m)	Treatment Segment		Control Segment	
	Left Bank (metric tons/yr)	Right Bank (metric tons/yr)	Left Bank (metric tons/yr)	Right Bank (metric tons/yr)
0.3	0.000	0.019	0.544	0.082
0.9	0.798	0.572	0.553	0.000
1.5	0.472	0.000	0.000	0.000

4.8 Critical Shear Stress

The stream at bankfull flow distributes a variety of different size particles from sand to gravel as shown in Table 4.10.

Table 4.10 Distribution of particle sizes at bankfull flow within the study site at Geronimo Creek.

Dominance	Particle Size Class (mm)
D_{16}	1.5
D_{35}	4
D_{50}	7
D_{84}	20
D_{95}	35
D_{100}	46

The D_{50} for the substrate in the riffle located at treatment 1 cross-section resulted in 19.3 mm which is particle size class gravel (Figure 4.7). Using Shield's Diagram (Leopold 1994), the

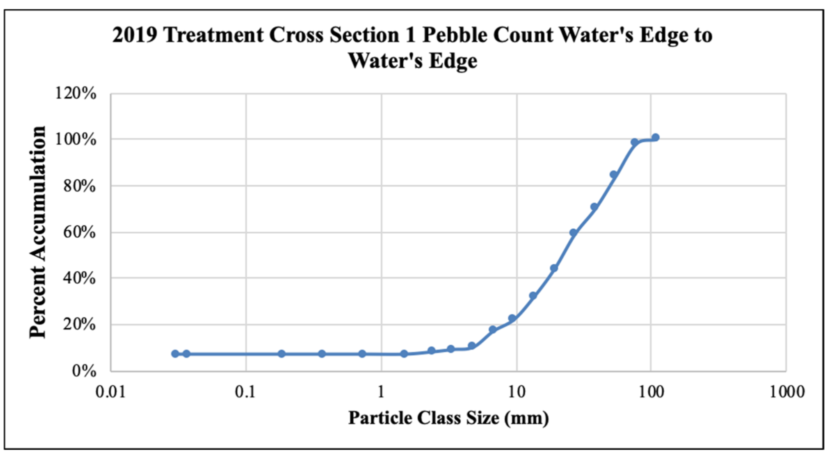

Figure 4.7 Particle size class for the substrate distribution of the study site at Geronimo Creek taken at a point bar located near the beginning of the study site.

corresponding critical shear stress was 1.76 kg/m^2. The resulting critical shear stress does not consider vegetation along the banks. To account for vegetation, a critical shear stress coefficient of 5.40, designated for sparse trees, was multiplied by the critical shear stress to result in a modified critical shear stress of 9.50 kg/m^2. The average cross-sectional shear stress was 5.13 kg/m^2. As a result, the vegetation increases the critical shear stress to exceed the shear stress reducing erosion along the banks.

5. DISCUSSION

When comparing 2018 to 2019 geomorphological data, discrepancies were noticed in the bankfull area. As a result of anthropogenic influences (e.g. the bridge upstream and the walking/biking path), the bankfull field indications were misguiding (e.g. slope break, change in particle size of substrate, exposed root hairs, vegetation line difference). Back calculations using the return period and corresponding precipitation adapted from Perica et al. (2018) with Geronimo Creek discharge for Seguin (Table 5.1) were used in eq. 3.8 to re-determine the bankfull discharge which typically occurs between the 1 to 2-year return period (Dunne & Leopold 1978).

Table 5.1 NOAA return period for Seguin, TX with its corresponding precipitation and Geronimo Creek discharge adapted from Perica et al. (2018).

Return Period	Precipitation (cm)	Discharge (cms)
0.5	4.76	7
1	7.70	25
1.4	9.16	40
1.5	9.49	44
2	10.08	63
5	13.39	175
10	16.64	361
25	21.64	921
50	26.16	1854
100	31.24	3720

When comparing the 2018 and 2019 geomorphological data using the Rosgen Classification of Streams, the channel morphed from a semi C-G to a complete G classification. The evolution from C to G indicates the deepening and widening of the channel as it moves upstream likely as a result of anthropogenic land cover change. The pebble count data from both years, showed a change from D_{50} of silt to D_{50} of gravel. The bar sample assessment confirmed that the dominant substrate for the study site was gravel.

After evaluating the BEHI values across all eight cross sections, it was determined that the left bank was prone to more erosion as a result of its location on the outside of a meander bend. When looking at the segments individually from year to year, the treatment segment had slightly better BEHI values in 2019 than in 2018. The slight improvement in values was a result of additional surface protection and root density from the newly established vegetation planted. The control segment values remained near the same for both years. The change in BEHI values in the segments during the approximate 1-year study were statistically different at the $p<0.10$ level based on the two independent samples t-test. The relationship of BEHI and NBS erosion predictions shows that if results are moderate to extreme for both assessments, then the stream will inevitably have erosion occurring on the banks. Evidence of the BEHI and NBS relationship was shown by the soil loss measured from the erosion pins.

The most soil loss along the banks occurred within 0.3 to 0.9 meters above the normal water level. The right bank had less erosion as a result of being located on the inside of the meander bend where in some cases accretion was observed (e.g. the point bar located near treatment cross-section 1). Soil loss was greatest among the left bank as a result of its location on the outside of the meander bend. The left bank totaled 78% of the total erosion for the entire study site. The treatment segment observed 0.68 metric tons of soil loss/year more than the control segment. This majority of the soil loss observed along the left treatment bank is attributed to a localized area of erosion at the beginning of the treatment segment where the soil possesses high clay content with small pieces of gravel. Plantings here survived but very slow growth was observed due to soil content that is harder for plant roots to penetrate.

Change within the average sediment load for the treatment and control segments were 26% reduction and 50% increase, respectively. The treatment segment reduced the sediment load from the storm events where as the control segment gained in sediment load. The vegetation modified critical shear stress exceeded the average bankfull shear stress by an excess of 4.37 kg/m^2. The excess means that erosion should be reducing as a result of vegetation. The coefficient used for the modified shear stress represents the relationship of healthy, mature sparsely populated woody species cover with a mature, healthy herbaceous layer. While the study site had several mature woody species, the understory was still in a transitioning state to healthier, but young vegetation. The study observed only the first year of newly established vegetation growth. Ideally, 2-3 years minimum of monitoring, following planting, should be documented for better observation of the indirect relationship of root growth with soil erosion in a more progressively healthier mature riparian stage.

6. CONCLUSION

The study site at Geronimo Creek has evolved from a C to a G stream, likely as a result of anthropogenic land cover change. After approximately one year of observation, the treatment segment had a larger soil erosion rate, but a reducing sediment load when compare to the control segment. Also, there was a statistical difference at the $p<0.10$ level in the BEHI analysis. The critical shear stress exceeded the bankfull shear stress indicating that erosion should be decreasing when modified by vegetation.

The study site needs several more years for the vegetation to become well-established and mature to enable possible observation of lower erosion rates and stabilized streambanks. To complete the study, monitoring of the riparian area should be performed at minimum another 1-3 years not only to observe sediment loads and erosion rates from well-established mature vegetation but to also observe more storm events of differing intensity and duration. Additionally, *in situ* testing of critical shear stress should be performed using jet testing to gain a more accurate measurement of the critical shear stress for the study site.

Stable vegetation is a fundamental part of the solution for stabilizing streambanks and NCD (Abernethy and Rutherfurd 1998; Beeson and Doyle 1995; Harman and Starr 2011; Polvi et al., 2014; Purvis and Fox 2016; and USDA NRCS 2007). As concluded by the study of the different assessments used, replanted native vegetation does effectively reduce the sediment load in the stream after approximately one year of study. To make this study more robust, however, several more years of data should be observed from more well-established mature plants to continue to monitor and better understand potential erosion and soil load reduction as the stream and its banks experience many types of storm frequencies and durations.

To further the research performed, these analyses should be conducted in other areas of the watershed to provide a collective view on the stream classification and erosion rate of Geronimo Creek. Several more BEHI and NBS data points along the creek could be used in performing an erosion prediction curve for the watershed providing potential erosion rate guidance for other similar watersheds in the region.

REFERENCES

Abernethy, Bruce, and Ian D. Rutherfurd. 1998. "Where Along a River's Length Will Vegetation Most Effectively Stabilise Stream Banks?" *Geomorphology* 23, no. 1: 55-57. doi: https://doi.org/10.1016/S0169-555X(97)00089-5.

Arguez, Anthony, Imke Durre, Scott Applequist, Russell S. Vose, Michael F. Squires, Xungang Yin, Richard R. Heim Jr., and Timothy W. Owen. 2012. NOAA's 1981-2010 U.S. Climate Normals: An Overview. *Bulletin of the American Meteorological Society* 93: 1687-1697. doi:10.1175/BAMS-D-11-00197.1

Arnold, Chester L., Paul J. Boison, and Peter C. Patton. 1982. "Sawmill Brook: An Example of Rapid Geomorphic Change Related to Urbanization." *The Journal of Geology* 90, no. 2: 155-166.

Baird, Rodger, Laura Bridgewater, American Public Health Association, American Water Works Association, Water Environment Federation. 2017. *Standard Methods for the Examination of Water and Wastewater*. 23rd ed: Washington D.C.: American Water Works Association.

Baker, David B., R. Peter Richards, Timothy T. Loftus, and Jack W. Kramer. 2004. "A New Flashiness Index: Characteristics and Applications to Midwestern Rivers and Streams." *Journal of the American Water Resources Association* 40, no. 2: 503-522. doi:10.1111/j.1752-1688.2004.tb01046.x

Baldigo, Barry P., Dana R. Warren, Anne G. Ernst, and Christiane I. Mulvihill. 2008. "Response of Fish Populations to Natural Channel Design Restoration in Streams of the Catskill Mountains, New York." *North American Journal of Fisheries Management* 28, no. 3: 954-969. doi: 10.1577/M06-213.1.

Bartley, Rebecca, Rex J. Keen, Aaron A. Hawdon, Peter B. Hairsine, Mark G. Disher, and A. E. Kinsey-Henderson. 2008. "Bank Erosion and Channel Width Change in a Tropical Catchment." *Earth Surface Processes and Landforms* 33, no. 14: 2174-2200. doi: 10.1002/esp.1678.

Beeson, C. E., and P. F. Doyle. 1995. "Comparison of Bank Erosion at Vegetated and Non-vegetated Channel Bends." *Journal of the American Water Resources Association* 31, no. 6: 983-990. doi: 10.1111/j.1752-1688.1995.tb03414.x.

Belmont, Patrick, Karen B. Gran, Shawn P. Schottler, Peter R. Wilcock, Stephanie S. Day, Carrie Jennings, J. Wesley Lauer et al. 2011. "Large Shift in Source of Fine Sediment in the Upper Mississippi River." *Environmental Science & Technology* 45, no. 20: 8804-8810. doi: 10.1021/es2019109.

Bernhardt, Emily S., Margaret A. Palmer, J. David Allan, G. Alexander, Katie A. Barnas, S. Brooks, J. Carr et al. 2005. "Synthesizing U.S. River Restoration Efforts." *Science* 308, no. 5722: 636. doi: 10.1126/science.1109769.

Blackport, Ray, Rob MacGregor, and Jack Imhof. 1995. *An Approach to the Management of Groundwater Resources to Protect and Enhance Fish Habitat*. Ontario, Canada: Canadian Manuscript Report of Fisheries and Aquatic Sciences. 2284: 70 p.

Chow, Ven T. 1959. *Open-channel Hydraulics*. Tokyo: McGraw-Hill Civil Engineering Series.

Davies, Neil S., and Martin R. Gibling. 2011. "Evolution of Fixed-Channel Alluvial Plains in Response to Carboniferous Vegetation." *Nature Geoscience* 4: 629. doi: 10.1038/ngeo1237.

Doll, Barbara A., Garry L. Grabow, Karen R. Hall, James Halley, William A. Harman, Gregory D. Jennings, and Dani E. Wise. 2003. Stream Restoration: a Natural-Channel-Design Handbook. NC Stream Restoration Institute, North Carolina State University, Raleigh.

Dunne, Thomas and Luna B. Leopold. 1978. *Water in Environmental Planning*. San Francisco: W.H. Freeman and Co.

Geronimo Creek Watershed Data Report. 2016. The Meadows Center for Water and the Environment.

Goel, Pradeep K., Ramesh P. Rudra, Bahram Gharbaghi, Samaresh Das, and Neelam Gupta. 2004. Pollutants Removal by Vegetative Filter Strips Planted with Different Grasses. ASAE/CSAI Annual International Meeting 042177. St. Joseph, Michigan: ASAE.

González, Eduardo, Anna A. Sher, Eric Tabacchi, Adrià Masip, and Monique Poulin. 2015. "Restoration of Riparian Vegetation: A Global Review of Implementation and Evaluation Approaches in the International, Peer-Reviewed Literature." *Journal of Environmental Management* 158: 85-94. doi: https://doi.org/10.1016/j.jenvman.2015.04.033.

Gustafson, David I., Katherine H. Carr, Timothy R. Green, Christophe Gustin, Russell L. Jones, and R. Peter Richards. 2004. "Fractal-Based Scaling and Scale-Invariant Dispersion of Peak Concentrations of Crop Protection Chemicals in Rivers." *Environmental Science & Technology* 38, no. 11: 2995-3003. doi: 10.1021/es030522p.

Hargrove, William L., Dewayne Johnson, Don Snethen, and Jan Middendorf. 2010. "From Dust Bowl to Mud Bowl: Sedimentation, Conservation Measures, and the Future of Reservoirs." *Journal of Soil and Water Conservation* 65, no. 1: 14A-17A. doi: 10.2489

Harman, William, Richard R. Starr. 2011. Natural Channel Design Review Checklist. US Fish and Wildlife Service, Chesapeake Bay Field Office, Annapolis, MD and US Environmental Protection Agency, Office of Wetlands, Oceans, and Watersheds, Wetlands Division. Washington, D.C. EPA 843-B-12-005

Henshaw, Patricia C., and Derek B. Booth. 2000. "Natural Restabilization of Stream Channels in Urban Watersheds." *Journal of the American Water Resources Association* 36, no. 6: 1219-1236. doi: 10.1111/j.1752-1688.2000.tb05722.x.

Julian, Jason P., and Raymond Torres. 2006. "Hydraulic Erosion of Cohesive Riverbanks." *Geomorphology* 76, no. 1: 193-206. doi: https://doi.org/10.1016/j.geomorph.2005.11.003.

Klein, Linda R., Stephen R. Clayton, J. Richard Alldredge, and Peter Goodwin. 2007. "Long-Term Monitoring and Evaluation of the Lower Red River Meadow Restoration Project, Idaho, U.S.A." *Restoration Ecology* 15, no. 2: 223-239. doi: 10.1111/j.1526-100X.2007.00206.x.

Lane, E.W. 1955. “The Importance of Fluvial Morphology in Hydraulic Engineering.” *Proceedings from the American Society of Civil Engineers*. 81, no. 745: 1-17.

Lenhart, Christian F., David J. Smith, Ann Lewandowski, Patrick Belmont, Larry Gunderson, and John L. Nieber. 2018. "Assessment of Stream Restoration for Reduction of Sediment in a Large Agricultural Watershed." *Journal of Water Resources Planning and Management* 144, no. 7: 04018032. doi: 10.1061/(ASCE)WR.1943-5452.0000908.

Leopold, Luna B., and William W. Emmett. 1976. "Bedload Measurements, East Fork River, Wyoming." *Proceedings of the National Academy of Sciences* 73, no. 4: 1000. doi: 10.1073/pnas.

Leopold, Luna B. 1994. *A View of the River.* Cambridge: Harvard University Press.

Ling, Ward, Mark McFarland, Debbie Magin, Loren Warrick, and Aaron Wendt. 2012. Geronimo and Alligator Creeks Watershed Protection Plan. Geronimo and Alligator Creeks Partnership.

Longwell, Chester Ray. 1946. "How Old is the Colorado River?" *American Journal of Science* 244, no. 12: 817-835.

Lowrance, Richard, Lee S. Altier, J. Denis Newbold, Ronald R. Schnabel, Peter M. Groffman, Judith M. Denver, David L. Correll, J. Wendell Gilliam, James L. Robinson, and Russell B. Brinsfield. 1997. "Water Quality Functions of Riparian Forest Buffers in Chesapeake Bay Watersheds." *Environmental Management* 21, no. 5: 687-712.

Lucchitta, Ivo. 2003. "Chapter 15 History of the Grand Canyon and of the Colorado River in Arizona." *Grand Canyon Geology,* edited by Stanley S. Beus and Michael Morales: 311-332. New York: Oxford University Press.

McClain, Charles D., Karen D. Holl, and David M. Wood. 2011. "Successional Models as Guides for Restoration of Riparian Forest Understory." *Restoration Ecology* 19, no. 2: 280-289. doi: 10.1111/j.1526-100X.2009.00616.x.

Miller, Ronald B., Garey A. Fox, Chad J. Penn, Stuart Wilson, Abigail Parnell, Rebecca A. Purvis, and Kelsey Criswell. 2014. "Estimating Sediment and Phosphorus Loads from Streambanks with and without Riparian Protection." *Agriculture, Ecosystems & Environment* 189: 70-81. doi: https://doi.org/10.1016/j.agee.2014.03.016.

Nagle, Gregory. 2007. "Evaluating Natural Channel Design Stream Projects." *Hydrological Processes* 21: 2539-2545. doi: 10.1002/hyp.6840.

National Oceanic and Atmospheric Administration (NOAA) National Centers for Environmental Information, Climate at a Glance: County Mapping, published December 2018, retrieved on January 28, 2019 from https://www.ncdc.noaa.gov/cag/

Perica, Sanja, Sandra Pavlovic, Michael St. Laurent, Carl Trypaluk, Dale Unruh, Orlan Wilhite. 2018. *Precipitation-Frequency Atlas of the United States*. 11. (2): Texas. National Oceanic and Atmospheric Administration Atlas 14.

Perucca, Eliana, C. Camporeale, and L. Ridolfi. 2007. "Significance of the Riparian Vegetation Dynamics on Meandering River Morphodynamics." *Water Resources Research* 43, no. 3. doi: 10.1029/2006WR005234.

Pimentel, David, C. Harvey, P. Resosudarmo, K. Sinclair, D. Kurz, M. McNair, S. Crist et al. 1995. "Environmental and Economic Costs of Soil Erosion and Conservation Benefits." *Science* 267, no. 5201: 1117-1123.

Polvi, Lina E., and Ellen Wohl. 2013. "Biotic Drivers of Stream Planform: Implications for Understanding the Past and Restoring the Future." *BioScience* 63, no. 6: 439. doi: 10.1525/bio.2013.63.6.6.

Polvi, Lina E., Ellen Wohl, and M. Merritt David. 2014. "Modeling the Functional Influence of Vegetation Type on Streambank Cohesion." *Earth Surface Processes and Landforms* 39, no. 9: 1245-1258. doi: 10.1002/esp.3577.

Purvis, Rebecca A., and Garey A. Fox. 2016. "Streambank Sediment Loading Rates at the Watershed Scale and the Benefit of Riparian Protection." *Earth Surface Processes and Landforms* 41, no. 10: 1327-1336. doi: 10.1002/esp.3901.

R Development Core Team. 2017. R: A Language and Environment for Statistical Computing. R Foundation for Statistical Computing, Vienna, Austria. <http://www.R-project.org/>. Accessed 21 April 2017.

Ren, Qingshui, Changxiao Li, Wenhang Yang, Hong Song, Peng Ma, Chaoying Wang, Rebecca L. Schneider, and Stephen J. Morreale. 2018. "Revegetation of the Riparian Zone of the Three Gorges Dam Reservoir Leads to Increased Soil Bacterial Diversity." *Environmental Science and Pollution Research* 25, no. 24: 23748-23763. doi: 10.1007/s11356-018-2333-3.

Rosgen, Dave L. 1996. *Applied River Morphology*. Pagosa Springs, Colorado: Wildland Hydrology.

Rosgen, Dave L. 2001. A Practical Method of Computing Streambank Erosion Rate. In Proceedings of the Seventh Federal Interagency Sedimentation Conference 1: II-9-II-15). Reno, NV: Subcommittee on Sedimentation.

Rosgen, Dave L. 2009. *Watershed Assessment of River Stability and Sediment Supply (WARSSS)*. 2nd ed. Fort Collins, Colorado: Wildlands Hydrology.

Smith, C., United States Federal Emergency Management Agency (FEMA), and L. Ritter. 2009. *Engineering with Nature: Alternative Techniques to Riprap Bank Stabilization*: FEMA.

Swanson, S. 2017. "Riparian Proper Functioning Condition Assessment to Improve Watershed Management for Water Quality." *Journal of Soil and Water Conservation* 72, no. 2: 168-182. doi: 10.2489/jswc.72.2168

Sweeney, Bernard W., and G. Blaine James. 2007. "Resurrecting the In-Stream Side of Riparian Forests." *Journal of Contemporary Water Research & Education* 136, no. 1: 17-27. doi: 10.1111/j.1936-704X.2007.mp136001003.x.

Tal, Michal, and Chris Paola. 2007. "Dynamic Single-Thread Channels Maintained by the Interaction of Flow and Vegetation." *Geology* 35, no. 4: 347-350. doi: 10.1130/G23260A.1.

Texas A&M Forest Service. 2018. “Texas Ecoregions: Blackland Prairie.” Accessed August 28, 2018. http://texastreeid.tamu.edu/content/texasEcoRegions/BlacklandPrairies/.

United States Census. 2017. “Quick Facts: Seguin and New Braunfels.” Accessed June 28, 2018. https://www.census.gov/quickfacts/fact/table/PST120217.

United States Department of Agriculture Natural Resources Conservation Service (USDA NRCS). 1977. Soil Survey of Guadalupe County, Texas.

United States Department of Agriculture Natural Resources Conservation Service (USDA NRCS). 2007. National Engineering Handbook, part 654. In *Stream Restoration Design*. NRCS, Washington, D.C.

United States Environmental Protection Agency (US EPA). 2016. Office of Water and Office of Research and Development. National Rivers and Streams Assessment 2008-2009: A Collaborative Survey (EPA/841/R-16/007). Washington, DC.

Walling, D. E., and B. W. Webb. 1985. "Estimating the Discharge of Contaminants to Coastal Waters by Rivers: Some Cautionary Comments." *Marine Pollution Bulletin* 16, no. 12: 488-492. doi: https://doi.org/10.1016/0025-326X(85)90382-0.

Wohl, Ellen, Brian P. Bledsoe, Robert B. Jacobson, N. Leroy Poff, Sara L. Rathburn, David M. Walters, and Andrew C. Wilcox. 2015. "The Natural Sediment Regime in Rivers: Broadening the Foundation for Ecosystem Management." *BioScience* 65, no. 4: 358. doi: 10.1093/biosci/biv002.

Wolman, M. G. 1954. "A Method of Sampling Coarse River-Bed Material." *Eos, Transactions American Geophysical Union* 35, no. 6: 951-956. doi: 10.1029/TR035i006p00951.

Yang, L., S. Jin, P. Danielson, C.G. Homer, L. Gass, S.M. Bender, A. Case et al. 2018. “A New Generation of the United States National Land Cover Database—Requirements, Research Priorities, Design, and Implementation Strategies” *Journal of Photogrammetry and Remote Sensing*, 146: 108–123. https://doi.org/10.1016/j.isprsjprs.2018.09.006.

APPENDIX A

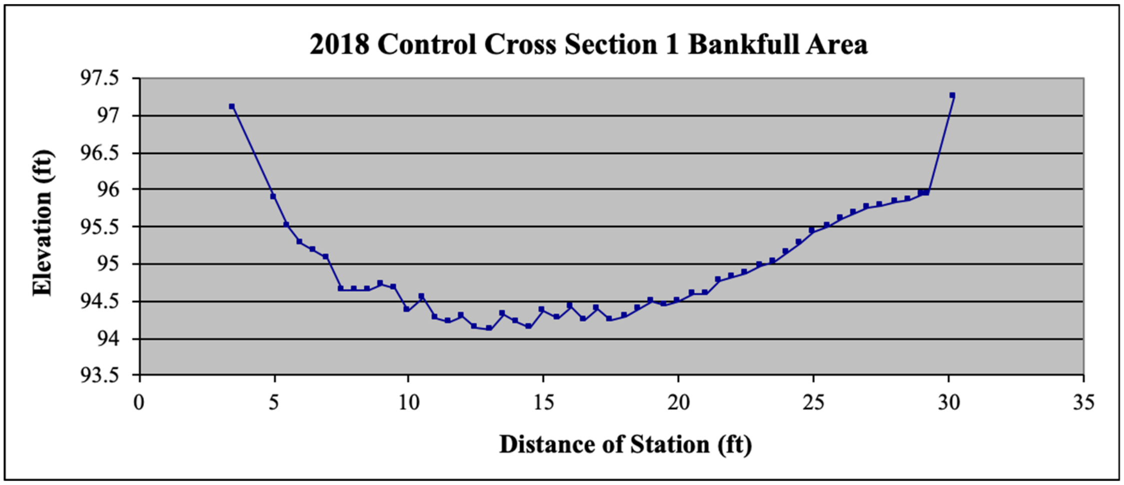

Figure A.1 2018 Bankfull Area of Control Cross Section 1.

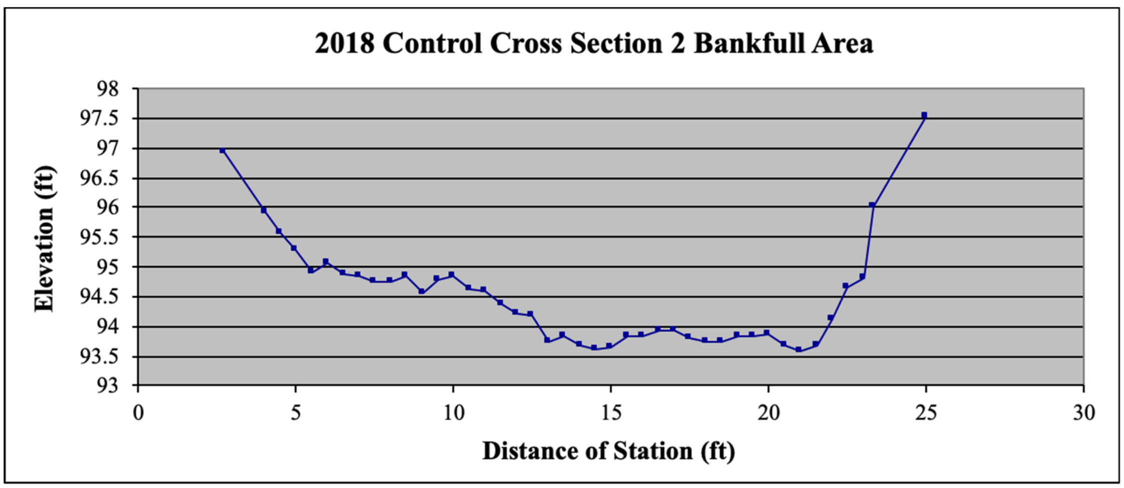

Figure A.2 2018 Bankfull Area of Control Cross Section 2.

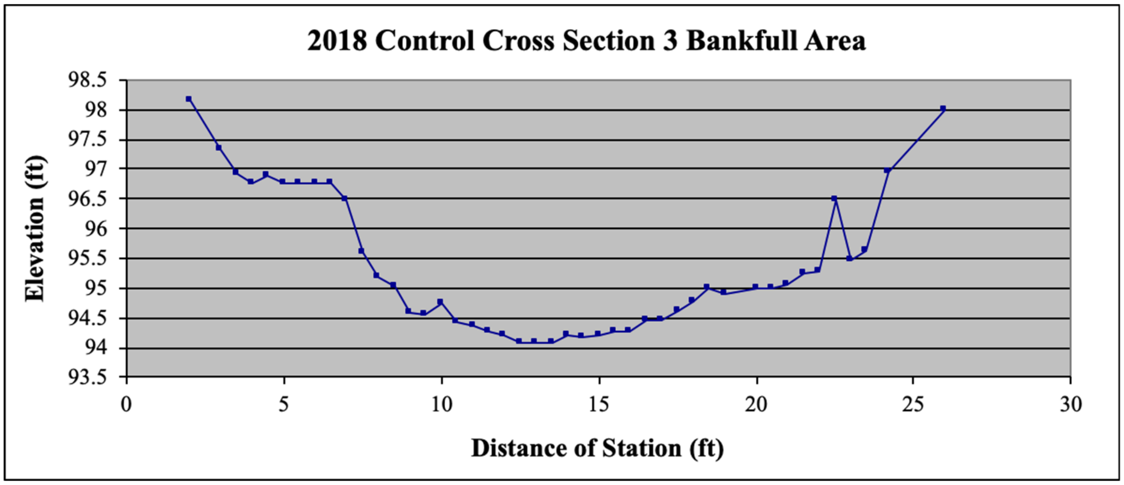

Figure A.3 2018 Bankfull Area of Control Cross Section 3.

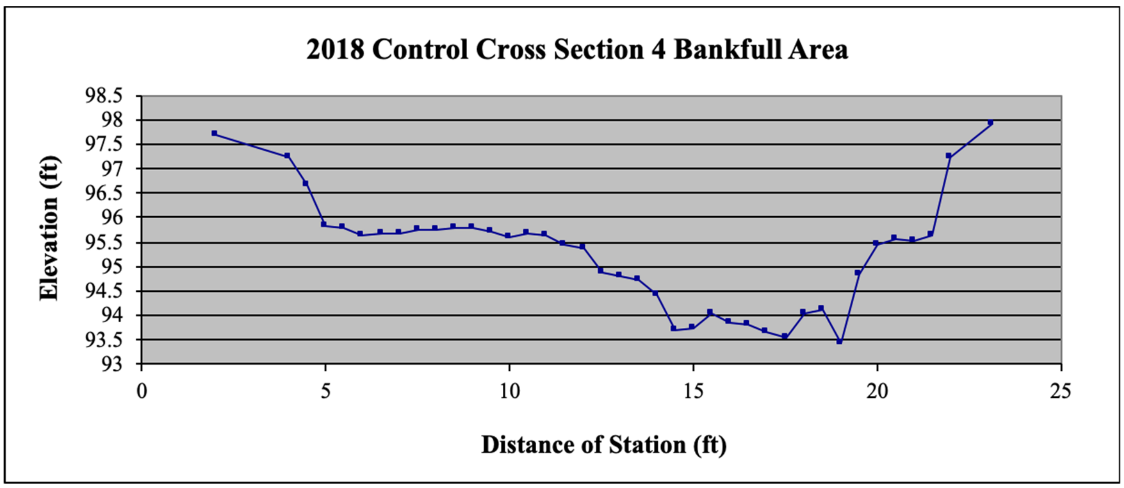

Figure A.4 2018 Bankfull Area of Control Cross Section 4.

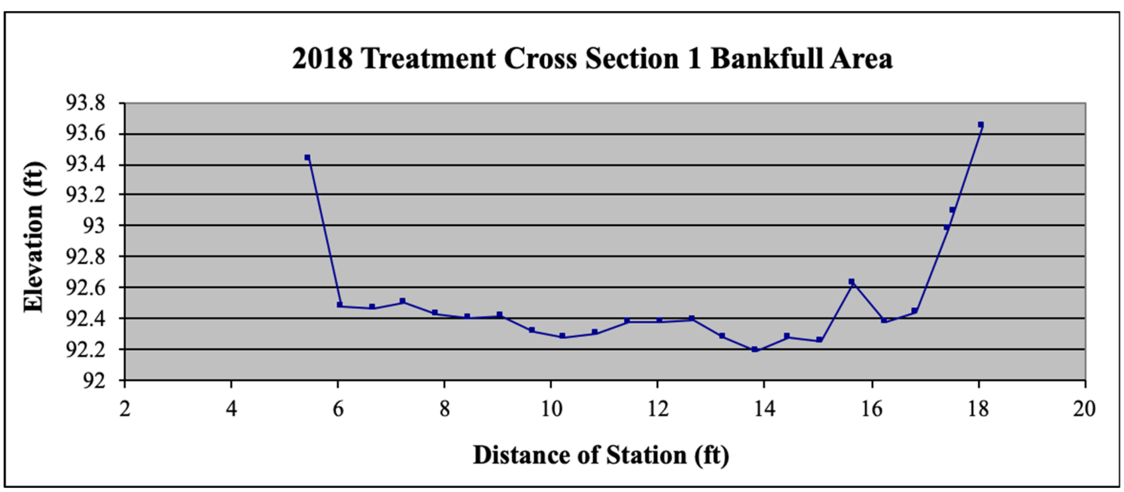

Figure A.5 2018 Bankfull Area of Treatment Cross Section 1.

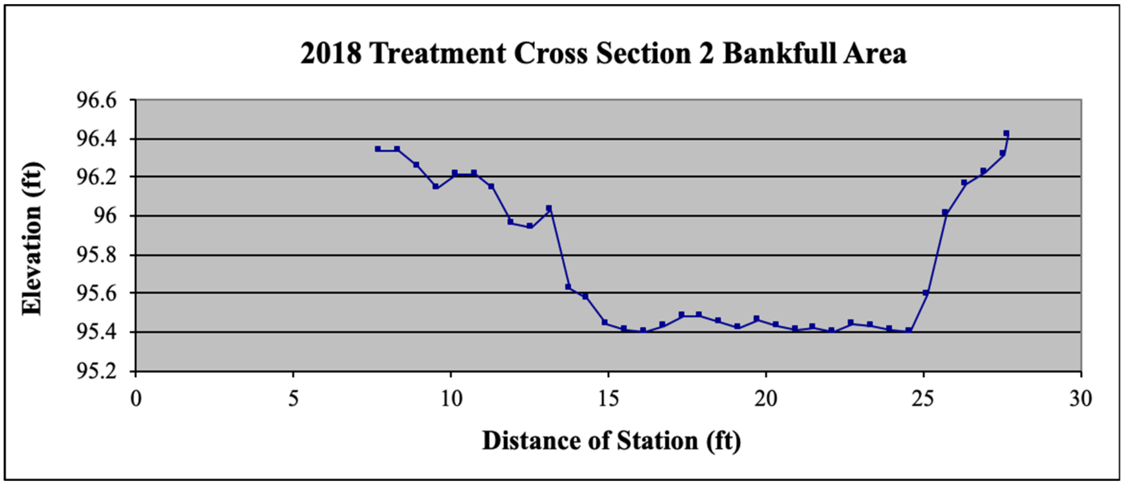

Figure A.6 2018 Bankfull Area of Treatment Cross Section 2.

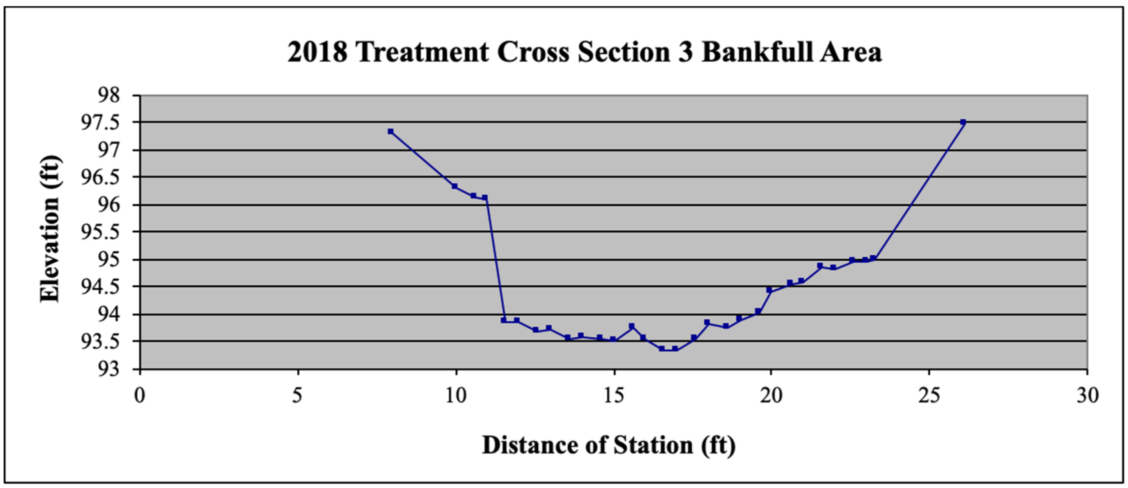

Figure A.7 2018 Bankfull Area of Treatment Cross Section 3.

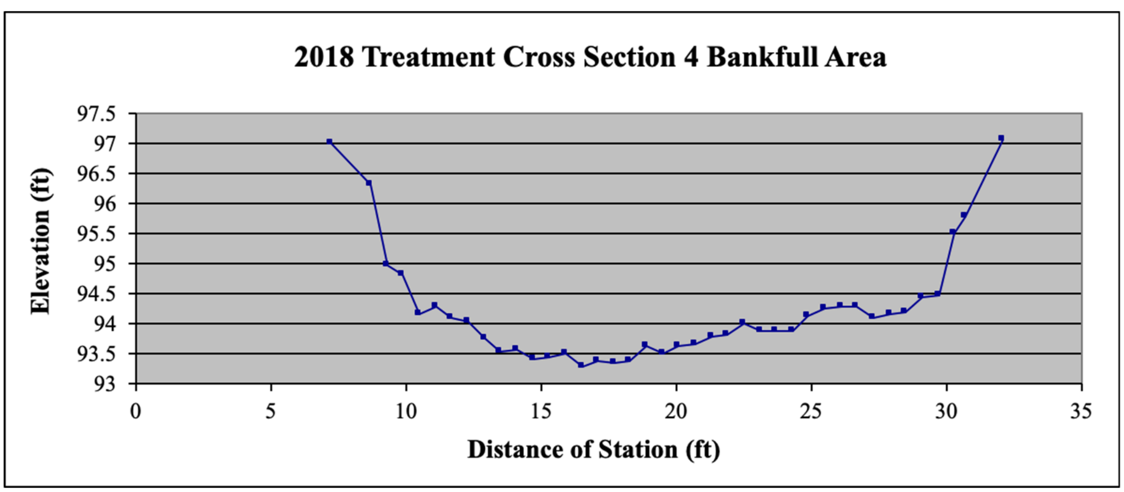

Figure A.8 2018 Bankfull area of Treatment Cross Section 4.

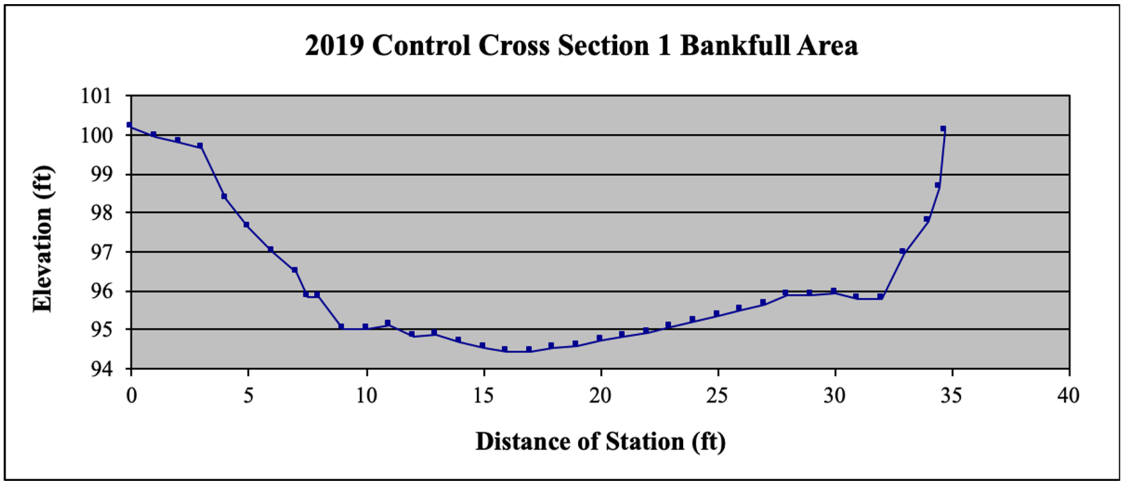

Figure A.9 2019 Bankfull Area of Control Cross Section 1.

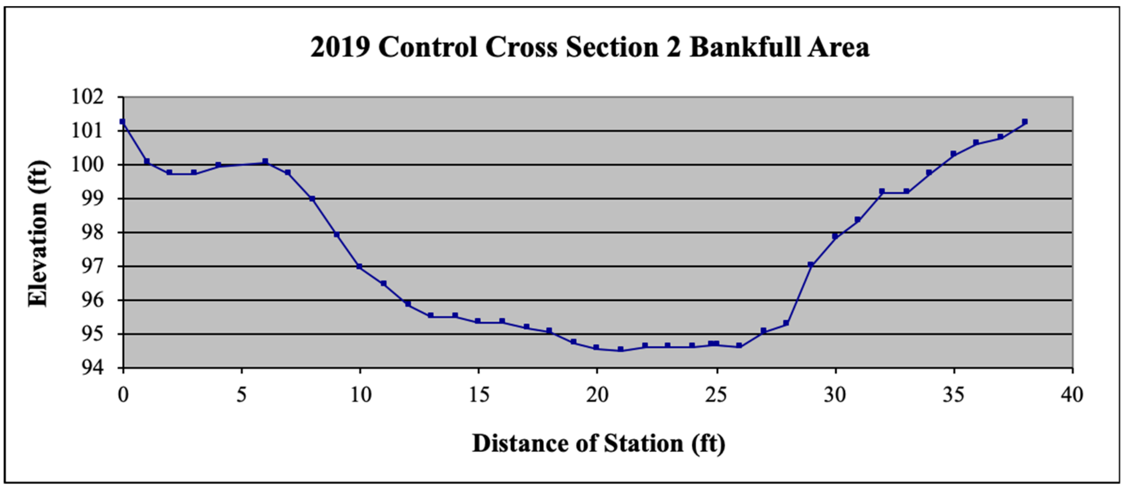

Figure A.10 2019 Bankfull Area of Control Cross Section 2.

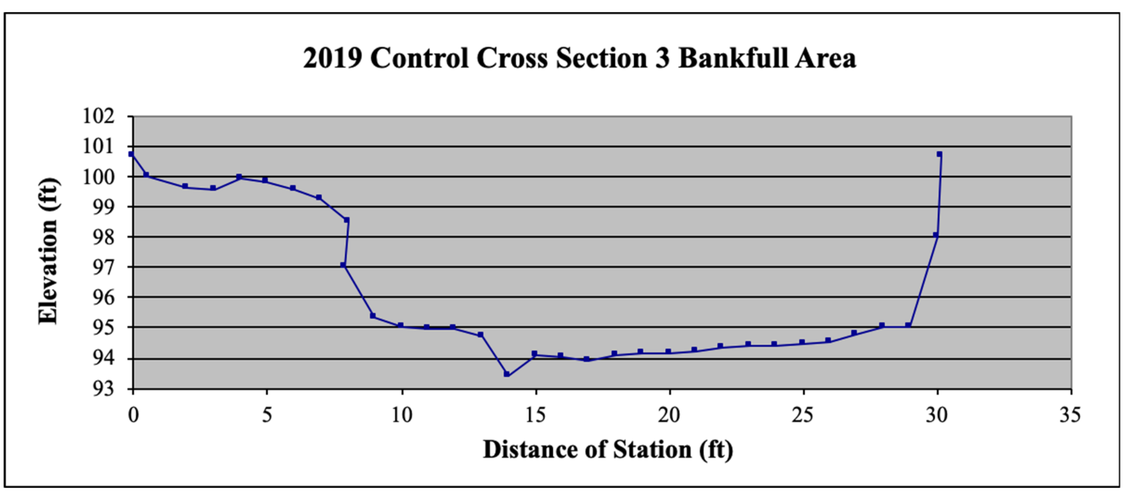

Figure A.11 2019 Bankfull Area of Control Cross Section 3.

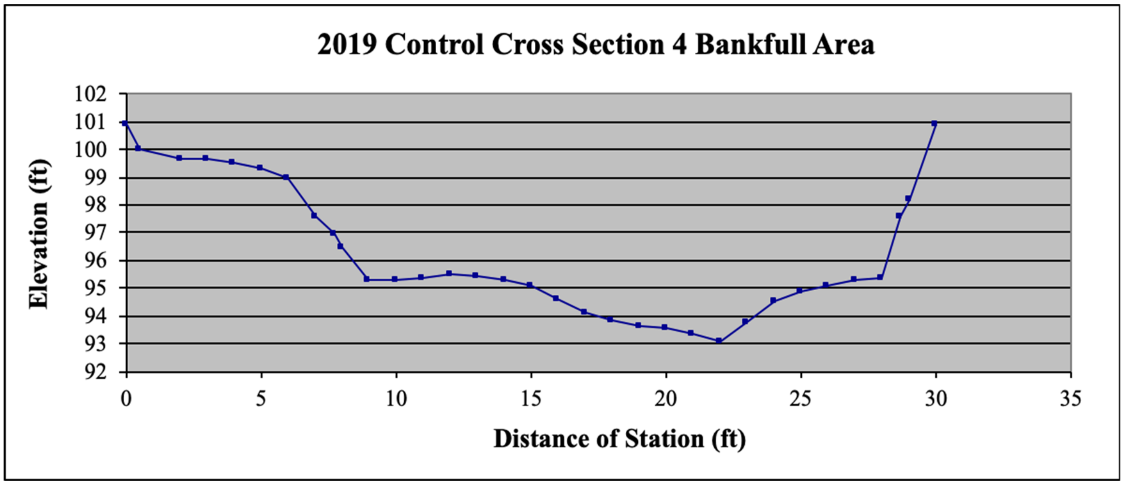

Figure A.12 2019 Bankfull Area of Control Cross Section 4.

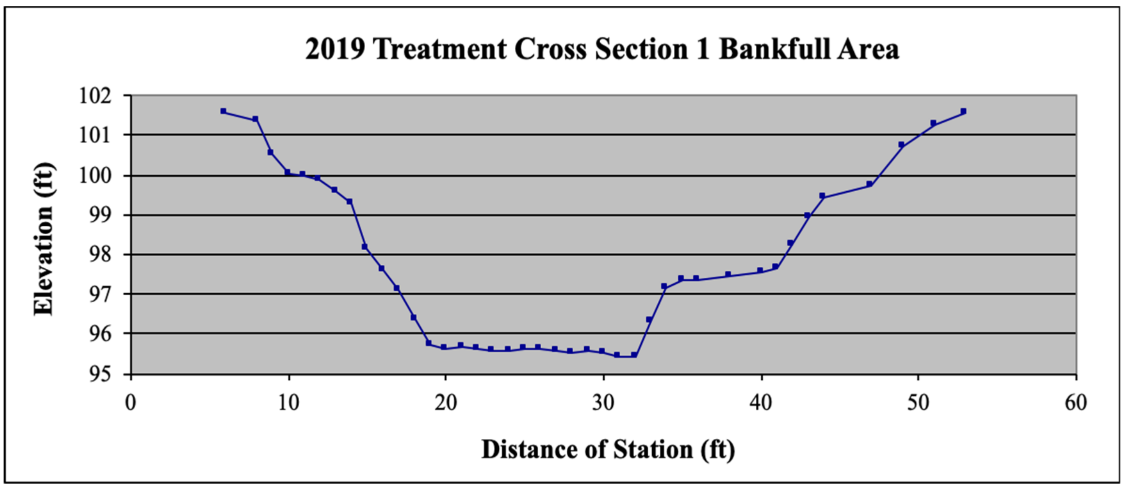

Figure A.13 2019 Bankfull Area of Treatment Cross Section 1.

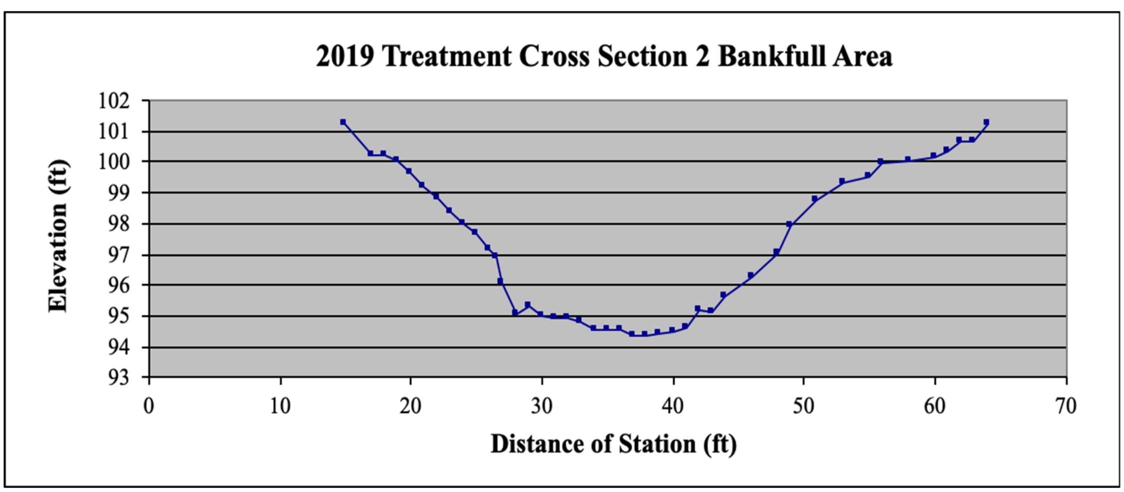

Figure A.14 2019 Bankfull Area of Treatment Cross Section 2.

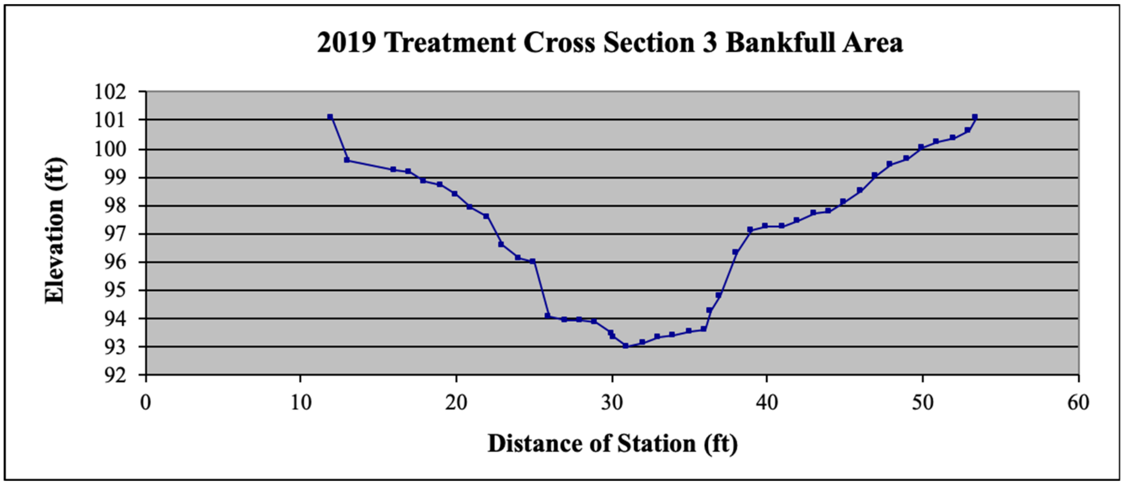

Figure A.15 2019 Bankfull Area of Treatment Cross Section 3.

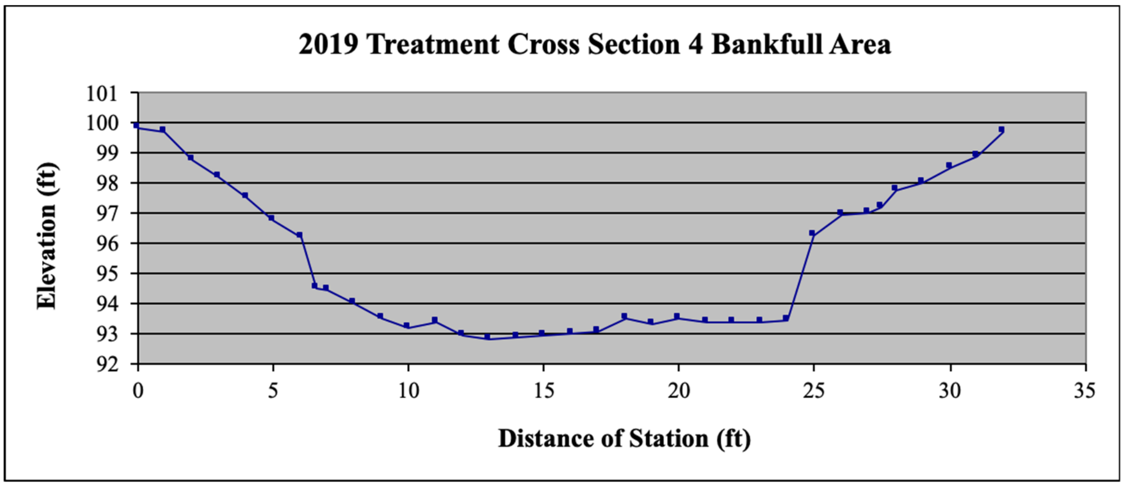

Figure A.16 2019 Bankfull Area of Treatment Cross Section 4.

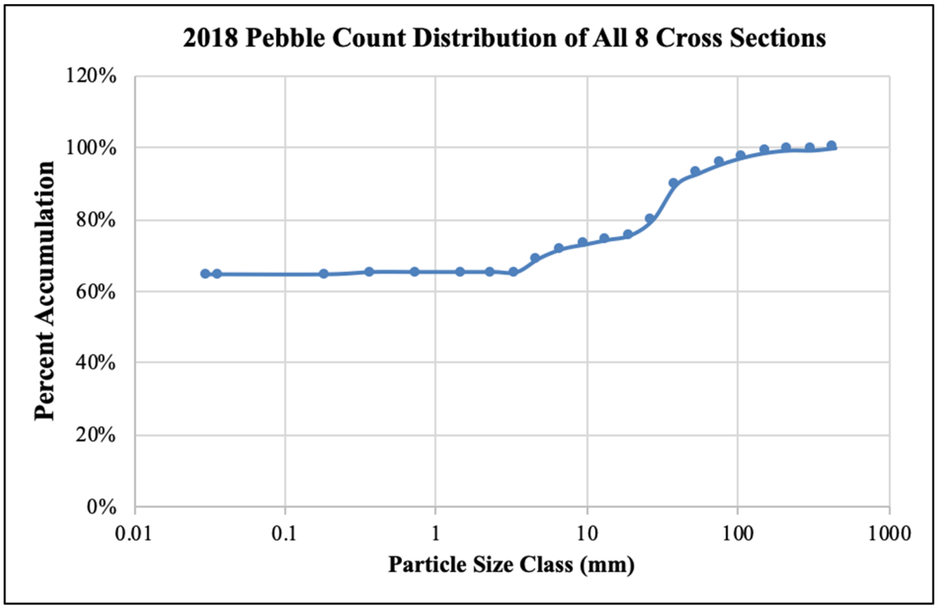

Figure A.17 2018 Pebble Count Distribution of All 8 Cross Sections.

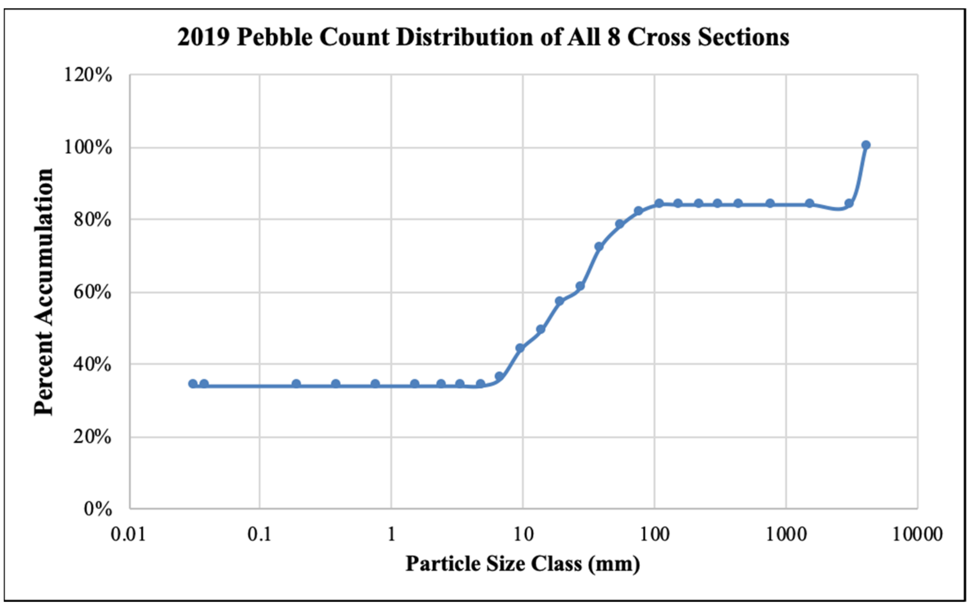

Figure A.18 2019 Pebble Count Distribution of All 8 Cross Sections.

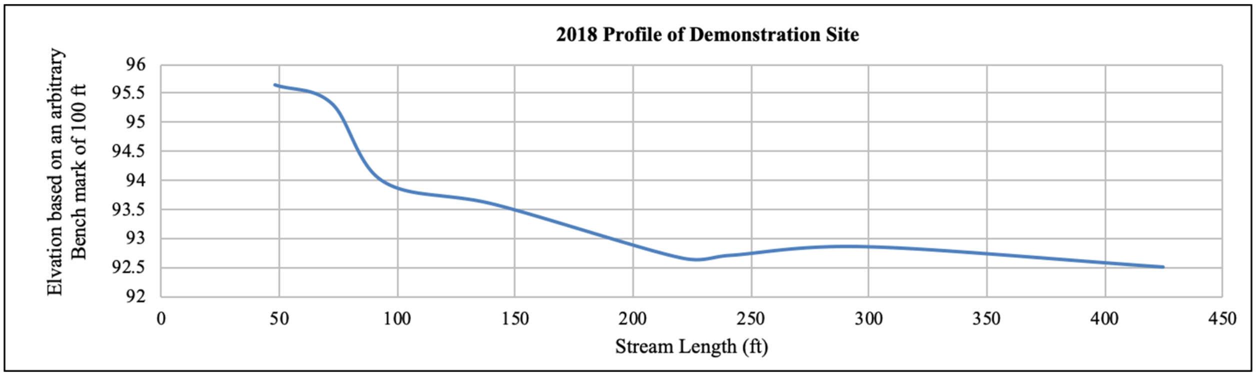

Figure A.19 2018 Profile Survey of the Thalweg for the Study Area.

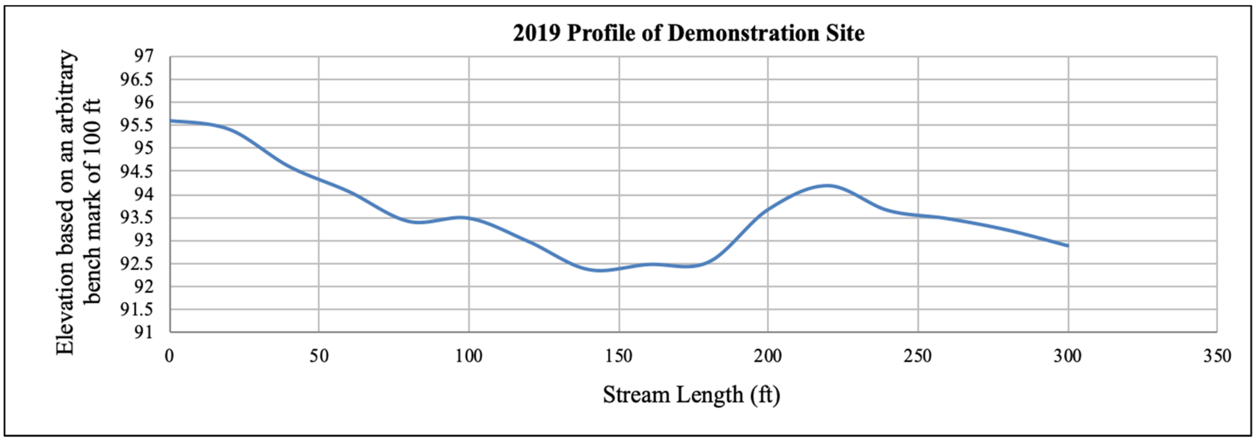

Figure A.20 2019 Profile Survey of the Thalweg for the Study Area.

APPENDIX B

Table B.1 2018 Geomorphological data for the control cross sections.

Parameters	Control 1 Bankfull Cross Section	Control 2 Bankfull Cross Section	Control 3 Bankfull Cross Section	Control 4 Bankfull Cross Section
Bankfull Area (ft^2)	59.0	53.3	66.7	48.7
Bankfull Width (ft)	26.7	22.3	24.0	21.1
Mean Bankfull Depth (ft)	2.2	2.4	2.8	2.3
Width/Depth Ratio	12.1	9.3	8.6	9.1
Width of Flood Prone Area (ft)	35.0	30.0	30.0	25.0
Entrenchment Ratio	1.3	1.3	1.3	1.2

Table B.2 2018 Geomorphological data for the control cross sections.

Parameters	Treatment 1 Bankfull Cross Section	Treatment 2 Bankfull Cross Section	Treatment 3 Bankfull Cross Section	Treatment 4 Bankfull Cross Section
Bankfull Area (ft^2)	12.7	12.8	47.7	70.4
Bankfull Width (ft)	12.7	20.0	18.1	24.9
Mean Bankfull Depth (ft)	1.0	0.6	2.6	2.8
Width/Depth Ratio	12.6	31.1	6.9	8.8
Width of Flood Prone Area (ft)	18.0	40.0	110.0	40.0
Entrenchment Ratio	1.4	2.0	6.1	1.6

Table B.3 2019 Geomorphological data for the control cross sections.

Parameters	Control 1 Bankfull Cross Section	Control 2 Bankfull Cross Section	Control 3 Bankfull Cross Section	Control 4 Bankfull Cross Section
Bankfull Area (ft^2)	144.8	147.6	143.2	144.1
Bankfull Width (ft)	34.7	38.0	30.4	30.0
Mean bankfull Depth (ft)	4.2	3.9	4.7	4.8
Width/Depth Ratio	8.3	9.8	6.4	6.2
Width of Flood Prone Area (ft)	50.0	50.0	35.0	40.0
Entrenchment Ratio	1.4	1.3	1.2	1.3
Wetted Perimeter (ft)	39.4	42.5	39.2	37.3

Table B.4 2019 Geomorphological data for the control cross sections.

Parameters	Treatment 1 Bankfull Cross Section	Treatment 2 Bankfull Cross Section	Treatment 3 Bankfull Cross Section	Treatment 4 Bankfull Cross Section
Bankfull Area (ft^2)	165.3	181.3	171.7	145.2
Bankfull Width (ft)	47.0	49.0	41.5	32.0
Mean bankfull Depth (ft)	3.5	3.7	4.1	4.5
Width/Depth Ratio	13.4	13.2	10.0	7.1
Width of Flood Prone Area (ft)	70.0	60.0	60.0	48.0
Entrenchment Ratio	1.5	1.2	1.4	1.5
Wetted Perimeter (ft)	54.2	67.4	58.9	37.9

Table B.5 BEHI values for the study banks on March 12, 2018.

Segment Type	Cross Section #	Bank Ht/ BKF Ht	Root Depth/ Bank Ht	Root Density %	Bank Angle	Surface Protection %	Bank Material (+5 pts)	BEHI Total
				BEHI Values				
Treatment Left	1	6.25	4.5	3.5	2.6	7	5	28.85
	2	10	1.9	2.8	1.9	3		19.6
	3	8.6	2.5	3.2	2.2	3.5		20
	4	8.2	1.9	5.2	2.7	4.4		22.4
Treatment Right	1	7.5	2.3	1	2.4	1.5	5	19.7
	2	7.9	2.5	3.6	2.6	3.5		20.1
	3	10	1.9	1.9	2.5	3.5	5	24.8
	4	10	2.5	4.4	2.5	3.5		22.9
Control Left	1	7.9	8.6	6.5	7	5.1		35.1
	2	7.9	8.6	6.5	7	5.1		35.1
	3	7.9	8.6	6.5	7	5.1		35.1
	4	7.9	6	4	5.5	6.5		29.9
Control Right	1	10	1.9	4.2	8.5	4.3		28.9
	2	10	1.9	4.2	3	4.3		23.4
	3	10	1.9	4.2	8.5	4.3		28.9
	4	10	1.25	5.9	4.9	5.1		27.15

Table B.6 BEHI values for the study banks on October 26, 2018.

Segment Type	Cross Section #	Bank Ht/ BKF Ht	Root Depth/ Bank Ht	Root Density %	Bank Angle	Surface Protection %	Bank Material (+5 pts)	BEHI Total
				BEHI Values				
Treatment Left	1	6.25	4.5	3.2	2.7	6.8	5	28.45
	2	10	1.9	1.9	1.9	2.2		17.9
	3	8.6	2.4	2.3	2.2	1.9		17.4
	4	8.2	1.9	4.2	2.7	3		20
Treatment Right	1	7.5	2.3	1	2.4	1.5	5	19.7
	2	7.9	2.5	3.6	2.6	3.5		20.1
	3	10	1.9	1.9	2.5	3.2	5	24.5
	4	10	2.5	3.9	2.5	3.5		22.4
Control Left	1	7.9	8.5	6.5	7	7		36.9
	2	7.9	8.6	6.5	7	5		35
	3	7.9	8.6	6.5	7	5.5		35.5
	4	7.9	5.9	4.2	5.5	6.5		30
Control Right	1	10	1.9	4.2	8.5	4.3		28.9
	2	10	1.9	4.2	3.2	4.3		23.6
	3	10	1.9	4.2	8.5	4.3		28.9
	4	10	1.25	5.9	5	7		29.15

Table B.7 BEHI values for the study banks on January 10, 2019.

Segment Type	Cross Section #	Bank Ht/ BKF Ht	Root Depth/ Bank Ht	Root Density %	Bank Angle	Surface Protection %	Bank Material (+5 pts)	BEHI Total
				BEHI Values				
Treatment Left	1	6.25	4.5	3.2	3.5	6.5	5	29
	2	10	1.9	1.9	1.9	3.5		19.2
	3	8.6	2.4	2.3	2.2	1.9		17.4
	4	8.2	1.9	4.2	2.7	3		20
Treatment Right	1	7.5	2.3	1	2.4	1.5	5	19.7
	2	7.9	2.5	3.6	2.6	3.5		20.1
	3	10	1.9	1.9	2.5	3.7	5	25
	4	10	2.5	3.9	2.5	3.5		22.4
Control Left	1	7.9	8.5	6.5	7	7.9		37.8
	2	7.9	8.6	6.5	7	5.3		35.3
	3	7.9	8.6	6.5	7	5.5		35.5
	4	7.9	6.6	5	5.5	7		32
Control Right	1	10	1.9	4.2	8.5	4.7		29.3
	2	10	2	4.2	3.2	4.7		24.1
	3	10	1.9	4.2	8.5	4.7		29.3
	4	10	1.25	5.9	5	7		29.2

Table B.8 BEHI values for the study banks on April 26, 2019.

Segment Type	Cross Section #	Bank Ht/ BKF Ht	Root Depth/ Bank Ht	Root Density %	Bank Angle	Surface Protection %	Bank Material (+5 pts)	BEHI Total
				BEHI Values				
Treatment Left	1	6.25	4.3	3.2	3.7	4.3	5	26.8
	2	10	1.8	1.9	1.9	3		18.6
	3	8.6	2.4	1.9	2.1	1		16
	4	8.2	1.9	3.9	2.7	1.5		18.2
Treatment Right	1	7.5	2.3	1	2.3	1	5	19.1
	2	7.9	2.5	3.2	2.7	2.8		19.1
	3	10	1.9	1.5	2.5	3.2	5	24.1
	4	10	2.5	3.9	2.5	1		19.9
Control Left	1	8.1	6.6	6.5	7	7.9		36.1
	2	7.9	7.9	5.9	5.9	5		32.6
	3	7.7	7.9	5.9	7	4.6		33.1
	4	7.5	6.8	5.1	5.5	5.7		30.6
Control Right	1	9.2	2.3	4.75	8.4	4.6		29.3
	2	10	2	3.9	3.1	2.8		21.8
	3	10	1.9	3.9	8.5	3.9		28.2
	4	10	1.3	5.7	5	4.3		26.3